

Dressing the Post-Newtonian two-body problem and Classical Effective Field Theory

Barak Kol and Michael Smolkin

*Racah Institute of Physics, Hebrew University
Jerusalem 91904, Israel*

E-mail: barak_kol@phys.huji.ac.il , smolkinm@phys.huji.ac.il

ABSTRACT: We apply a dressed perturbation theory to better organize and economize the computation of high orders of the 2-body effective action of an inspiralling Post-Newtonian gravitating binary. We use the effective field theory approach with the non-relativistic field decomposition (NRG fields). For that purpose we develop quite generally the dressing theory of a non-linear classical field theory coupled to point-like sources. We introduce dressed charges and propagators, but unlike the quantum theory there are no dressed bulk vertices. The dressed quantities are found to obey recursive integral equations which succinctly encode parts of the diagrammatic expansion, and are the classical version of the Schwinger-Dyson equations. Actually, the classical equations are somewhat stronger since they involve only finitely many quantities, unlike the quantum theory. Classical diagrams are shown to factorize exactly when they contain non-linear world-line vertices, and we classify all the possible topologies of irreducible diagrams for low loop numbers. We apply the dressing program to our Post-Newtonian case of interest. The dressed charges consist of the dressed energy-momentum tensor after a non-relativistic decomposition, and we compute all dressed charges (in the harmonic gauge) appearing up to 2PN in the 2-body effective action (and more). We determine the irreducible skeleton diagrams up to 3PN and we employ the dressed charges to compute several terms beyond 2PN.

Contents

1. Introduction and Summary	1
2. Dressed perturbation theory in CLEFT	5
2.1 Factorizable diagrams	6
2.2 Dressed charge and propagator	7
2.3 Equivalence of perturbation theories	10
2.4 The Schwinger-Dyson recursive integral equation in CLEFT	12
2.5 Irreducible 2-body skeletons	15
3. Dressing the 2-body Post-Newtonian problem	16
3.1 Effective action and Feynman rules	16
3.2 Dressed charges	18
3.3 Skeletons for 2PN and 3PN	25
3.4 Computing beyond 2PN	27
A. Master integrals	33

1. Introduction and Summary

Gravitational wave observatories (see for example the reviews [1] and references therein) demand knowledge of the waveform emitted by an inspiralling binary system of compact objects. Fully Generally Relativistic numerical simulations can now simulate such waveforms - see the review [2] and references therein. Yet, as always, an analytic treatment is complementary and improves insight, especially into the functional dependence of the results on the parameters. A *perturbative* analytic treatment is possible in two limits. The first is the Post-Newtonian (PN) approximation, and it holds whenever the velocities are small compared with the speed of light, or equivalently through the virial theorem whenever the separation between the compact objects is much larger than their Schwarzschild radii. The second limit is that of an extreme mass ratio. In this paper we shall concentrate on the PN approximation which is always valid at the initial stages of any inspiral.

The computation of the effective 2-body action in PN was a subject of considerable research over the last decades and the current state of the art is its determination up to order 3.5PN, as summarized in the review [3] (see also the recent [4]). Another approach, the effective field theory (EFT) approach to this problem was suggested by Goldberger and Rothstein (2004) [5], where more traditional GR methods are replaced by field theoretic tools including Feynman diagrams, loops and regularization. In particular [5] reproduced the 1PN effective action (known as Einstein-Infeld-Hoffmann) within the EFT approach. In

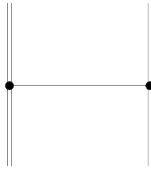


Figure 1: The diagram which represents the Newtonian potential interaction mediated through the Newtonian scalar field ϕ . The notations will be fully defined later in section 3.

[6, 7] the metric components in the Post-Newtonian, non-relativistic limit were conveniently decomposed into a scalar Newtonian potential, a gravito-magnetic 3-vector potential and a symmetric 3-tensor. These fields were termed collectively “fields of Non-Relativistic Gravitation (NRG fields)”, and the derivation of 1PN was shown to further simplify. In [8] the 2PN expression was reproduced within the effective field theory approach together with NRG fields.

Other recent developments related to either PN or the EFT approach include: dissipative effects and effective horizon degrees of freedom [9, 10]; thermodynamics of caged black holes [11, 12] through the EFT approach [13, 6, 14]; EFT [15] and Hamiltonians [16, 17] for rotating point-particles; tidal effects for compact objects [18, 19]; approximate solutions for higher dimensional black object including rings [20] and blackfolds [21]; a mechanized EFT computation for 2PN [22]; “De-Turek” gauge for numerical relativity [23]; and finally radiation reaction and waves within the EFT approach [24, 25].

The computation of order 2PN [8] demonstrates a proliferation in the number of diagrams: from 4 at 1PN to 21 at 2PN, and furthermore the number is expected to continue and grow at the next order. Clearly, it would be useful to have an improved perturbative expansion. In this paper we shall present a new method to better organize the calculation and economize it. The basic idea is to recognize recurring sub-diagrams which physically describe “dressed” charges and propagators. The simplest example is furnished by the Newtonian potential $G m_1 m_2 / |r_1 - r_2| \subset S_{eff}$ which belongs to order 0PN. This term is associated with the diagram in figure 1. At higher orders there is a class of diagrams of the form shown in figure 2 where the point masses are replaced by dressed energy distributions defined on the top row of figure 3

$$m_i \delta(x_i - r_i) \rightarrow \rho_{dr}(x_i - r_i) \quad (1.1)$$

and the bare propagator is replaced by the dressed (relativistic) one defined on the bottom of figure 3

$$\frac{1}{k^2} \delta(\Delta t) \rightarrow G(k, \Delta t) . \quad (1.2)$$

The same sub-diagrams which define the dressed energy distribution and appear in the calculation of the dressed Newtonian interaction (figure 2) appear also in other diagrams. It makes sense to record the values of these sub-diagrams and later re-use them. This is the basic idea of the dressed perturbation theory.

In addition, the dressing procedure is shown to economize the calculation in a more significant way as follows. We find that the dressed couplings satisfy a certain recursive

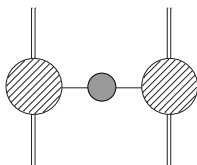
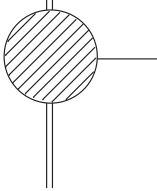


Figure 2: A class of diagrams that we interpret as the Newtonian potential interaction between *dressed* energy distributions of each body through a dressed propagator. The dark blobs represent any sub-diagram with an arbitrary number of vertices on the world-line and a single external leg for the Newtonian potential. There are no bulk loops, as always in classical physics. The light blob represents any sub-diagram with two external legs of the Newtonian potential, which amounts to a propagator with an arbitrary number of retardation insertions.

$$\int dt \int \frac{d^3\mathbf{k}}{(2\pi)^3} \rho(t, \mathbf{k}) \phi(t, -\mathbf{k}) :=$$



$$G(\mathbf{k}, \Delta t) :=$$


Figure 3: The diagrammatic definition of the dressed energy distribution (top) and the dressed propagator (bottom). The dressed energy distribution is defined through the one point function for ϕ in the presence of a single source (after stripping external propagators), while the dressed propagator is defined through the full two point function for ϕ .

integral equation schematically described in figure 4. A perturbative expansion of the solution to this equation equals an infinite sum of diagrams, and in this sense it encodes many diagrams. This is nothing but the classical version of the Schwinger-Dyson equations which were first written in the context of quantum electro-dynamics [26]. Yet the current classical version is of a higher practical value compared to its quantum counterpart since it does not involve the infinitely many dressed bulk vertices.

Some discussions of classical versions of the Schwinger-Dyson equations appeared already, yet they all appear to consider a significantly different context. [27] studied unequal time correlation functions of a non-equilibrium classical field theory, while [28] aims at giving a construction of the local algebras of observables in quantum gauge theories.

The paper is divided into two parts. In section 2 we describe and discuss the dressed perturbation theory for a general classical (effective) field theory, while in section 3 we apply it to the Post-Newtonian theory. We start in section 2 by considering a simple

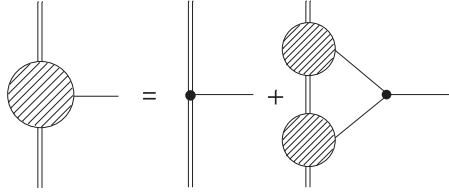


Figure 4: A schematic diagrammatic representation of the Schwinger-Dyson recursive integral equation satisfied by the dressed couplings. More details are given in the body of the paper.

scalar classical field theory coupled to point-like particles as the context for introducing the required dressing concepts. In subsection 2.1 we characterize the fully factorizable diagrams before turning in subsection 2.2 to our main definition, that of the dressed quantities. In subsection 2.3 we define the dressed perturbation theory and assert that it is equivalent to the bare theory.

In subsection 2.4 we explain the recursive integral equation à la Schwinger-Dyson and comment on its relation with related concepts. We close the general theory section in subsection 2.5 with a classification of irreducible skeletons at low loop numbers - diagrams which are neither factorizable nor do they include dressed sub-diagrams.

In section 3 we apply these concepts of dressing theory to better organize and economize the two-body Post-Newtonian (PN) effective action. In subsection 3.1 we set up the problem by displaying the Post-Newtonian effective action and the associated Feynman rules. In subsection 3.2 we explicitly compute the three charges in PN. The charge which couples to the gravitational field is the energy-momentum tensor, and since the gravitational field naturally decomposes in the PN limit into three NRG-fields the source decomposes too into three corresponding parts: the energy density, the momentum density and the stress. These charges are computed both in k -space and in position space up to the order required to reproduce the 2PN results, and the stress is determined to one additional order.

In 3.3 we analyze qualitatively the diagrams relevant to the computation of the two-body effective action. Starting with 0PN and making our way to order 2PN we explain how some of the diagrams can be expressed through dressed charges, and which diagrams can be generated by the integral equation. Up to order 2PN only a single (non-tree) diagram is found to be irreducible. We confirmed that the known 2PN effective action is reproduced after incorporating our expressions for the dressed charges from the previous subsection. While thus far almost all the computations are related to the known [3] 2PN effective action which was already reproduced within the EFT approach with NRG fields in [8], here we list all the skeletons required for the computation of 3PN, thereby indicating the road-map for organizing the 3PN computation. In subsection 3.4 we convincingly demonstrate the utility of our method by computing certain novel 3PN and 4PN diagrams.¹ Finally, in appendix A we collect some useful integrals.

¹The computed first Post-Minkowskian approximation [29] includes information about a certain class of diagrams to arbitrarily high PN orders, which are different however from the ones we compute here.

2. Dressed perturbation theory in CLEFT

In this section we define a dressed perturbation theory in the general CLEFT (Classical Effective Field Theory) context, namely for any classical non-linear field theory coupled to point-like sources.

In order to illustrate the main ideas in a simple setting we consider a scalar field model. The generalization to an arbitrary CLEFT is straightforward and will be spelled out at the end of subsection 2.2 on p. 9.

Consider the following bulk action

$$S_{\text{bulk}}[\phi] = \int d^4x \left[-\frac{1}{2}(\vec{\nabla}\phi)^2 + \frac{1}{2c^2}\dot{\phi}^2 - \frac{\alpha}{6}\phi^3 \right] \quad (2.1)$$

for a scalar field ϕ with propagation speed c and coefficient of cubic interaction α , where ϕ couples to any point particle of mass m and charge q through

$$S_p = -(m - q) \int d\tau - q \int e^{\phi(x(\tau))} d\tau, \quad (2.2)$$

$d\tau$ is the proper time element and the particles will be assumed non-relativistic $d\vec{x}/d\tau \ll c$ (or even static in part of the discussion). *The total action* for a many body system is

$$S = S_{\text{bulk}} + \sum_a S_{p,a}, \quad (2.3)$$

where $S_{p,a}$ is the world-line action (2.2) of the a 'th particle characterized by m_a, q_a .

Let us briefly discuss the considerations for choosing this form of the action. The retardation term proportional to $1/c^2$ is considered as a small perturbation in the non-relativistic limit and represents a general small perturbation of the quadratic term. The term proportional to α was chosen to represent any non-linear interaction. The interaction term $-q \int \exp(\phi(x(\tau)))$ includes the charge coupling $-q \int \phi(x(\tau))$ together with some representative non-linear terms (this exponential form of the interaction appears in Post-Newtonian theory, for example).

The bulk theory (2.1) has a vacuum at $\phi = 0$ and we consider the perturbation theory around it. As usual, we note that while this vacuum is unstable, it could be stabilized by adding a mass term to S_{bulk} , and it could even be made a global minimum through the addition of a quartic term in the potential.

In this paper we study the *two-body problem* rather than the seemingly more general *many body problem* since it is the simplest and currently the most interesting case. The generalization to the many body problem seems straight forward.

The *Feynman rules* involving ϕ are shown in figure 5. They are standard except for the CLEFT conventions which makes them real – vertices are read from the action and propagators are given schematically by $-1/S_2$ where S_2 is the quadratic part of the action. See [6] for the original definition and full detail.

The two body effective action is defined by

$$S_{eff}[x_1, x_2] := S[x_1, x_2, \phi(x_1, x_2)] \quad (2.4)$$

$$\begin{array}{cc}
\frac{t_1 \quad \mathbf{k} \quad t_2}{\quad} = +\frac{1}{\mathbf{k}^2} \delta(t_1 - t_2) & \frac{t_1 \quad \overset{t}{\times} \quad t_2}{\frac{\partial}{\partial t_1} \quad \frac{\partial}{\partial t_2}} \\
\\
\begin{array}{c} \diagup \\ \bullet \\ \diagdown \end{array} \quad = -\alpha & \\
\\
\begin{array}{c} \parallel \\ \bullet \\ \parallel \end{array} \quad = -q \sqrt{1-v^2} & \begin{array}{c} \parallel \\ \bullet \\ \diagup \\ \diagdown \end{array} \quad = -q \sqrt{1-v^2}
\end{array}$$

Figure 5: The Feynman rules involving ϕ for the static scalar field theory whose action is given by (2.3). The rules describe: the propagator and the quadratic perturbation vertex – retardation (top), the cubic bulk vertex (middle), and the world-line vertices (bottom) where the ellipsis stand for additional non-linear world-line vertices. Hereafter k denotes a spatial wave-number.

where the RHS represents the action (2.3) evaluated on the solution $\phi = \phi(x_1, x_2)$ given the particle trajectories $x_1(\tau_1)$, $x_2(\tau_2)$. The effective action is known to be equal to the sum of all connected Feynman diagrams made out of ϕ propagators with arbitrary bulk vertices and world-line vertices but without loops of propagating fields (such classically forbidden loops are allowed quantum mechanically).

2.1 Factorizable diagrams

There are several possible paths to classical dressed perturbation theory. We shall build it from first principles and later discuss its relations with both the quantum version and the standard classical theory.

The main idea is to economize the perturbation theory by identifying certain recurring sub-diagrams. Before we proceed to the more essential, dressed sub-diagrams we discuss a stronger and simpler form of reduction, namely factorizable diagrams.

A Feynman diagram is called *factorizable* whenever the expression which it represents factorizes (into a product of factors), each one corresponding to a sub-diagram. An example is shown in figure 6. In CLEFT we have the interesting property that *a diagram of the 2-body effective action is factorizable if and only if it contains a Non-linear world-line (NL-WL) vertex*, where a NL-WL vertex is a vertex with more than a single bulk field.

Indeed, if a diagram contains a NL-WL vertex then since quantum loops are not allowed, each leg of the vertex generates a separate sub-diagram. Conversely, a connected²

²All the diagrams of the 2-body action are connected by definition.

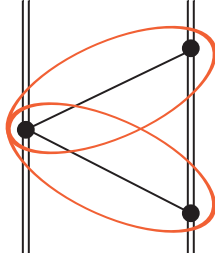


Figure 6: An example of a factorizable diagram (the simplest). The two factors are circled (in red) and they intersect in a NL-WL vertex. A diagram of this type appears at 1PN – see figure 23.

factorizable diagram necessarily factorizes at a vertex. A bulk vertex would not serve since wave-number conservation couples between all its legs.³

2.2 Dressed charge and propagator

Following our discussion of factorization we proceed to consider only diagrams without any NL-WL vertices. Any non-factorizable diagram contains various sub-diagrams. We wish to further economize the perturbation theory by identifying in a unique and natural way a class of sub-diagrams which repeatedly show up at high orders of the two body effective action. We shall call them “dressed sub-diagrams”. We start with constructive definitions and an explanation of the name’s origin, to be followed by a more abstract characterization through an equivalence of perturbation theories which serves to explain the rational behind the definitions.

Definitions

- The *dressed charge of the particle*, $\rho_{dr}(k, t)$ is defined diagrammatically through figure 7 (top). The dressed charge is an infinite sum of sub-diagrams, where each summand will be called a *dressed charge sub-diagram*.
- The *dressed propagator*, $G_{dr}(k, \Delta t)$ is defined diagrammatically through figure 7 (bottom). Each summand in the definition will be called a *dressed propagator sub-diagram*.

Let us inspect these definitions. In equations $\rho_{dr}(r)$ is defined through

$$\rho_{dr}(r, t) := \Delta\Phi(r, t) = \int d\tau q \delta^{(4)}(x - x(\tau)) + \frac{1}{2}\alpha \Phi^2 + \partial_t^2 \Phi \quad (2.5)$$

where the second equality is a differential equation which together with retarded boundary conditions defines $\Phi(r, t)$, the full solution for the field ϕ in presence of the given source

³In CLEFT we cannot have a factorizable diagram such as the “figure 8” diagram in ϕ^4 theory, since we cannot have k conservation for any strict subset of propagators leaving the bulk vertex, as each propagator connects to a distinct world-line vertex (or vertices) where k is arbitrary.

$$\int dt \int \frac{d^3 \mathbf{k}}{(2\pi)^3} \rho(\mathbf{k}, t) \phi(-\mathbf{k}, t) := \text{diagram} = \text{diagram} + \text{diagram} + \dots$$

$$G(\mathbf{k}, t_2 - t_1) := \text{diagram} = \text{diagram} + \text{diagram} + \text{diagram} + \dots$$

Figure 7: The diagrammatic definition of the dressed charge distribution (top) as the one point function for ϕ in the presence of a single source and the dressed propagator (bottom) as the full two point function for ϕ in vacuum. Retardation vertices are forbidden on the external leg of the dressed charge.

$$\Phi(t, \mathbf{k}) := \text{diagram}$$

Figure 8: The diagrammatic representation for the value of the field in the presence of the point-particle source. The only difference with the definition of the dressed charge in figure 7 (top) is an added propagator on the external leg.

world-line. This equation is equivalent to the diagrammatic definition since Φ is given diagrammatically by figure 8, and hence in k -space $\Phi(k, t) = -\rho_{dr}(k, t)/k^2$ from which (2.5) follows in position space.

The dressed charge describes the apparent particle charge (distribution) at long distances. It arises from the non-linear interactions of the scalar field which “dress” the point charge, and is useful for studying the dynamics of a system composed of several such particles. The term which we use, “dressed” charge (and propagator) is standard terminology in quantum field theory (see for example [30]) as well as in classical field theory. For completeness we would like to mention some related terms. The first is renormalization, where like here one replaces a bare quantity by a scale-dependent renormalized quantity which is defined through the divergences of the same sub-diagrams.⁴ Another related term is

⁴The idea of renormalization in the PN context appeared already in the literature. [31] associated renormalization with the regularization of certain divergences which appear in the particle’s effective action at order 3PN. [5] studied the same divergences from the EFT approach and in particular they computed the renormalization of the energy-momentum tensor of a static particle up to 2 loops. Later [32] also studied

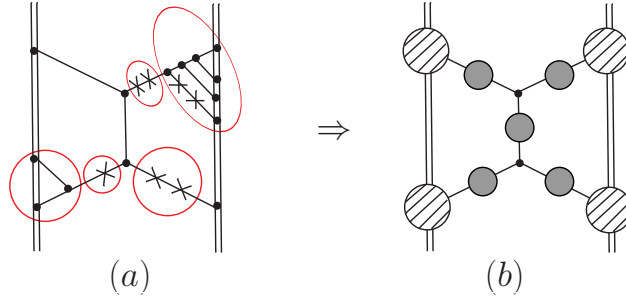


Figure 9: An example for the correspondence between diagrams of the bare theory, such as (a) and the corresponding dressed diagram (b). Note a standard subtlety: retardation insertions are allowed inside a dressed charge vertex, but not on its external leg. See text for further discussion.

resummation where one discusses partial sums of diagrams.

The equation form of the dressed propagator is

$$\begin{aligned}
 G_{dr} &= \frac{1}{\square} = \frac{1}{k^2 + \partial_t^2/c^2} = \frac{1}{k^2} \frac{1}{1 + \partial_t^2/(c^2 k^2)} = \\
 &= \frac{1}{k^2} \left(1 - \frac{1}{c^2 k^2} \partial_t^2 + \frac{1}{c^4 k^4} \partial_t^4 + \dots \right)
 \end{aligned} \tag{2.6}$$

where the last equality is a representation of the series on the left of figure 7 (bottom), while the previous expressions can be considered to be a closed form summation of that series.

Physically, in this field theory and also in PN the dressed propagator is nothing but the fully relativistic propagator. However, this need not be the case in general.

Example. To illustrate these ideas let us discuss an example. A detailed application to the Post-Newtonian theory will be given in section 3.

Consider the 6-loop Feynman diagram in figure 9(a) which contributes in the bare theory to the 2-body effective action. It has five dressed sub-diagrams (circled) – two dressed charges and three dressed propagators. Note that all the world-line vertices of each dressed charge belong to *one and the same* point particle. Note also that retardation vertices are allowed inside the dressed charge but not on its external leg. Upon replacing the dressed sub-diagrams by dressed vertices and propagators we obtain the diagram’s skeleton⁵ in (b). The resulting diagram is only two-loop. The other loops were absorbed by the dressed charges. Note that the 3-loop dressed charge sub-diagram includes in it other dressed sub-diagrams, but these are not maximal.

Generalization. So far we worked in a simple setting of a cubic scalar field model. Here we shall indicate how the definitions given above for the dressed sub-diagrams generalize to a general field theory.

the renormalization of the energy-momentum tensor.

⁵This term will be further discussed and defined in the next subsection.

In the scalar field theory we had a single dressed vertex and a single dressed propagator. In a general Classical field theory interacting with point-like particles we have a dressed charge for each field. For the dressed charge to be non-trivial the bulk theory must be interacting.

The dressed propagator in a general field theory is labeled by any two fields that can “mix”. In case the fields do not mix then we have a single dressed propagator for each field. For the dressed propagator to be non-trivial we need the quadratic Lagrangian to decompose into a leading part and a perturbation, so that the leading part will determine the bare propagator, while the small part will determine the two-vertex. The dressed propagator will then be proportional to the inverse of the full quadratic Lagrangian. We note that one may choose to diagonalize the dressed propagator and accordingly redefine the fields such that there will be no mixing through dressed propagators.

2.3 Equivalence of perturbation theories

We proceed to define a dressed perturbation theory, which is equivalent to the original one, but somewhat more economic.

Definition. A Feynman diagram which includes a non-trivial dressed sub-diagram of the form shown in figure 7 (*dressing sub-diagram*) will be called *dressing-reducible*. Otherwise it will be called *dressing-irreducible*.

Definition. The *dressed perturbation theory* is defined as follows

- Figure 10 shows the changes in Feynman rules relative to the original theory (figure 5).
- Only dressing-irreducible diagrams are allowed.

The original perturbation theory will be distinguished from the dressed one by referring to it as *bare*.

Property – *The bare and dressed perturbation theories are equivalent:* each diagram of the bare theory is included exactly once in a dressed diagram.

This property is analogous to a standard one holding for dressed actions in QFT, and we shall outline a proof. Given a bare diagram we claim that its maximal dressed sub-diagrams are unique. We find the uniqueness property to be quite apparent when one thinks about it, but we shall not attempt to provide here a proof, as it seems tedious. Given the decomposition we replace the dressed sub-diagrams by propagators and vertices of the dressed theory according to figure 10. The resulting reduced diagram is called *the skeleton* of the original diagram. The uniqueness of decomposition implies now that each bare diagram is included once and only once in the dressed perturbation theory, and hence the two are equivalent.

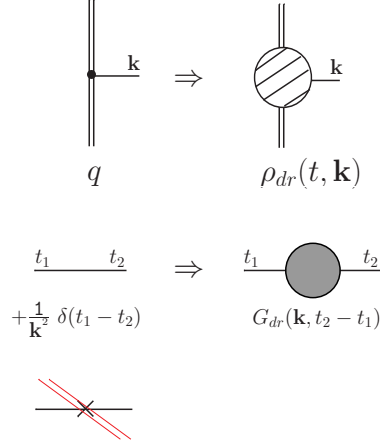


Figure 10: The dressed Feynman rules contain changes relative to the bare Feynman rules in figure 5. The bare world-line vertex (charge) Feynman rule changes into the dressed one, the bare propagator changes into the dressed one, and the retardation rule is omitted. The rest of the rules remain unchanged.

Discussion. Before proceeding to describe another property of the dressed theory, namely, the integral equation, let us pause to discuss some aspects of the definitions and property above.

Rational behind definitions. The decomposition into a skeleton with blobs which represent dressed sub-diagrams is natural in a practical, computational sense. When computing a diagram, the dressed sub-diagrams are almost inevitably evaluated on the way, by their nature. Hence it is computationally natural to prepare a list of dressed sub-diagrams and their value, in order to avoid their repeated evaluation, which is exactly what the dressed theory does.

Yet, the computational argument alone does not fix our definitions of the dressed sub-diagram. *The characterizing property is precisely the equivalence property above*, namely that the dressed perturbation theory is equivalent to the bare one, or in other words, *the dressed theory is self-sufficient or autonomous*. We claim (again without proof) that this property can be used to *derive* our definitions.

Analogy with effective action in Quantum Field Theory (QFT). The ideas above are analogous to those of the effective action in standard QFT. There one collects all the 1-particle-irreducible (1PI) diagrams into the effective action and then allows in the perturbative expansion only tree diagrams of the effective action. In both cases it is important that the decomposition is unique – any diagram can be uniquely divided into 1PI sub-diagrams which allow a reduction to a tree skeleton.

Relation of the dressed sub-diagrams with the “dressed source” in standard QFT. The two notions are essentially the same. Note however that unlike some cases, for us it is important that the dressed charge sub-diagrams are only those where all world-line vertices belong to one and the same point particle.

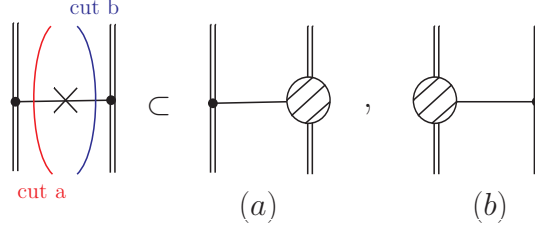


Figure 11: An over-counting problem with an alternative definition of the (non-static) dressed perturbation theory, as discussed in the text.

Our notion of the dressed propagator is also essentially the same as the dressed propagator and the associated field strength renormalization in standard QFT. The 2-vertex in CLEFT is the “self energy” (the 1PI two point function), and (2.6) is essentially the standard QFT relation between the self energy and the dressed propagator. The difference is that in QFT many diagrams can contribute to the self energy (actually normally they are infinitely many corresponding to an arbitrary number of possible loops) while in CLEFT the 2-point vertex is read directly from the Lagrangian.

Why is the dressed propagator necessary? Consider doing away with the definition of the dressed propagator by allowing the dressed vertex sub-diagrams to include retardation vertices on the external leg. In the classical theory this would actually work in all but one important class of diagrams, that of the dressed Newtonian interaction – figure 2, where the correspondence between the bare and dressed diagrams would break. For example, consider the diagram in figure 11. There are two distinct ways to cut the diagram into sub-diagrams, the cuts being denoted by a,b. Accordingly this diagram is doubly counted in the putative dressed theory, thereby disqualifying it. This is all the better since the dressed propagator is an appealing physical concept which we would not want to lose anyway.

2.4 The Schwinger-Dyson recursive integral equation in CLEFT

In this section we shall describe a second property of the dressed perturbation theory: certain recursive relations which generally take the form of integral equations. We start by considering the static limit of the scalar theory (2.3) where the idea is simpler to illustrate and later we refine it to include the general non-static case.

Recall the definition of $\rho_{dr}(r)$ in figure 7.

Property. *The dressed quantities satisfy recursive relations.* In the static limit $\rho_{dr}(r)$ satisfies the recursive relation which is shown diagrammatically in figure 12. Its equation form reads

$$-\int \frac{d^3k}{(2\pi)^3} \rho_{dr}(k) \phi(-k) = -q \phi|_{\vec{r}=0} + \frac{\alpha}{2} \int \frac{d^3k}{(2\pi)^3} \int \frac{d^3k_1}{(2\pi)^3} \frac{\rho_{dr}(k_1)}{k_1^2} \frac{\rho_{dr}(k-k_1)}{(k-k_1)^2} \phi(-k) . \quad (2.7)$$

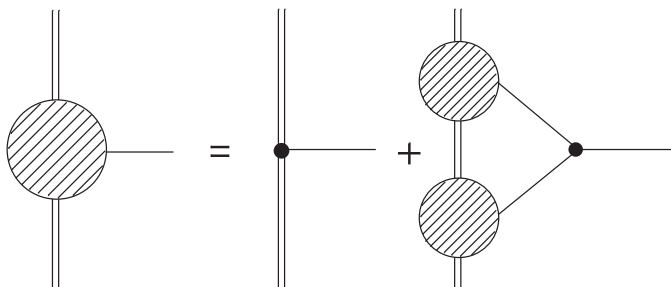


Figure 12: The diagrammatic representation of the recursive integral equation satisfied by the dressed charge in the static limit.

After factoring out $\int d^3k \phi(-k)/(2\pi)^3$ we are left with the following integral equation for $\rho_{dr}(k)$

$$\rho_{dr}(k) = q - \frac{\alpha}{2} \int \frac{d^3k_1}{(2\pi)^3} \frac{\rho_{dr}(k_1)}{k_1^2} \frac{\rho_{dr}(k-k_1)}{(k-k_1)^2}. \quad (2.8)$$

Given a small α the integral equation can be solved perturbatively in α by expanding $\rho_{dr}(k) = \sum \alpha^n \rho^{(n)}(k)$. The zeroth order is given by $\rho^{(0)}(k) = q$, the first order is given by $\rho^{(1)}(k) = \frac{1}{2} \int d^3k_1/(2\pi)^3 \alpha \frac{q}{k_1^2} \frac{q}{(k-k_1)^2}$ and so on. This iterative solution of the integral equation is precisely equivalent to the diagrammatic expansion in figure 7 (because they both compute the same quantities, namely $\rho^{(n)}(k)$).

The advantage of the integral equation over the diagrammatic expansion is that it is shorter and economizes the computation by avoiding the need to identify all the necessary diagrams and compute them. Some readers may benefit from the following analogy: the relation between the recursive relation and the full diagrammatic expansion is analogous to the relation between defining a function through a differential equation and defining it through the corresponding power series which solves the differential equation.

The non-static case. Once we restore time dependence into the action (2.3) we expect the dressed propagator to have a role in the recursive relations as well. First, it has a recursive relation of its own given diagrammatically by figure 13 (bottom). In this case the recursive relation is actually algebraic rather than integral, and hence the closed form solution (2.6) exists. Secondly, the recursive relation for the dressed vertex (figure 12) is refined to include the dressed propagator and is now given by figure 13 (top).

We now proceed to make several comments.

- The recursive relation (figures 12,13 and equation 2.8) can be considered as inherited from its quantum version (see for example [33]), but there are interesting differences. As it is, figure 12 does not hold in *quantum* field theory ⁶ because there can be additional ϕ propagators connecting the two blobs on the RHS. Since such additional propagators would create a closed loop of propagating fields it is forbidden in CLEFT.

⁶except for the tree diagram limit of course.

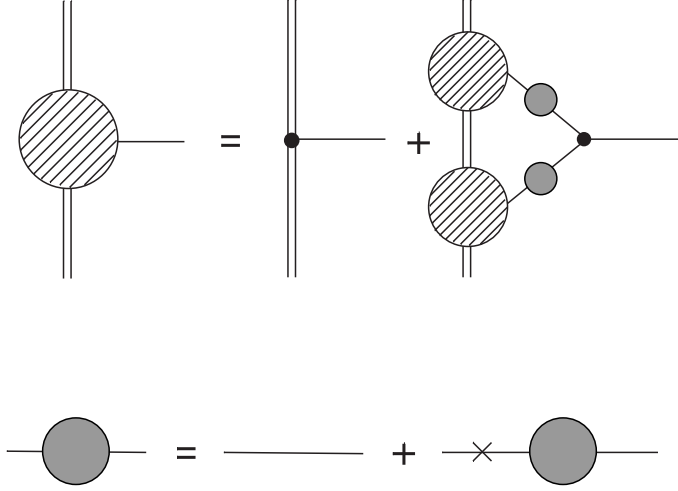


Figure 13: A diagrammatic representation of the full set of (the two) recursive equations satisfied by the dressed charge (top) and propagator (bottom) in the general, non-static case. Note a change in the recursive relation for the dressed charge relative to the static equation in figure 12.

In order for the recursive integral relations to apply in the quantum case one must generalize them to include the dressed bulk vertices yielding the celebrated Schwinger-Dyson equations [26]. However, as stated in several textbooks the practical usefulness of the quantum version is rather limited since more and more Green’s functions with more external legs participate in the equations as the order is increased ⁷ while in CLEFT the equations are more practical exactly because there are only a finite number of dressed quantities.

- The dressed mass $\rho_{dr}(r)$ is closely related to the field profile $\Phi(r)$ generated by the point-like source. Indeed, each one of them is sufficient to determine the other through (2.5). While $\rho_{dr}(r)$ satisfies an integral equation, $\Phi(r)$ satisfies a “mirror” differential equation, namely the equation of motion given by the second equality in (2.5). The perturbative expansion of the integral equation is dual in turn to the perturbative expansion of the differential equation into some sort of a power series (which will generally include log factors as well).
- Relation with the beta function. The recursive integral equation (2.8, and figures 12,13) determines $\rho_{dr}(k)$ and so does the beta function. Yet, the two equations are different as the beta function is a first order differential equation for $d\rho_{dr}/d\log(k)$. Therefore it must be that the beta function equation is a special or limiting case

⁷“From the point of view of making a practical calculation we have accomplished little; the unknown quantities ... have been expressed in terms of yet another unknown...” [33], “... the system involves an infinite hierarchy of equations ... their usefulness is limited” [34].

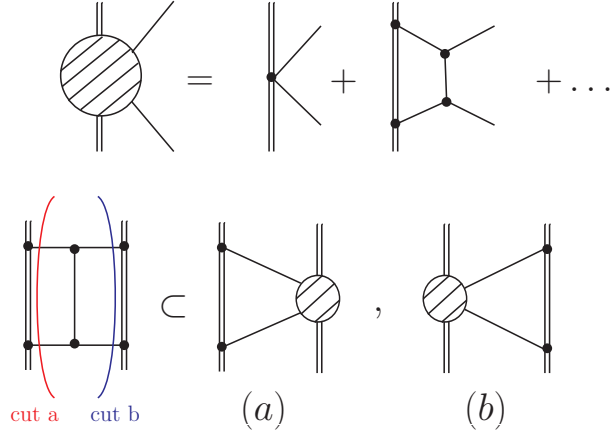


Figure 14: The top line shows a possible definition for a 2-field dressed world-line vertex. The second line demonstrates the over-counting problem which occurs. The bare diagram on the left can be cut into sub-diagrams in two different ways denoted (a) and (b).

(whose precise definition will not be pursued here) when the leading behavior of ρ_{dr} is logarithmic in k .

2.5 Irreducible 2-body skeletons

Consider the non-linear world-line vertices (NL-WL vertices) in the scalar action (2.3), namely vertices with more than a single bulk field. Our definition of the dressed charge concerns a world-line vertex with a single bulk field. It is possible to generalize the definition of the dressed vertex to any number of bulk fields, such as the 2-field vertex shown on the top line of figure 14. In this way one may define a *fully dressed one body effective action*.

However, for the purpose of computing the 2-body effective action *we use only the dressed charges (and propagators) and for the NL-WL vertices we use the bare vertices rather than the dressed ones* because they would have created a problem: the decomposition of diagrams would not have remained unique (just as in our discussion around figure 11). For example, the diagram on the second row of figure 14 can be decomposed in two *different* ways by the two shown cuts, and that corresponds to doubly counting this diagram in the putative fully dressed perturbation theory.

Recall (subsection 2.1) that non-linear world-line vertices are interesting for another, complementary property: *a diagram of the 2-body effective action is factorizable if and only if it contains a Non-linear world-line vertex*. From this perspective the above-mentioned issue with using dressed WL-NL vertices is all the better since there is no need for dressing – all diagrams with NL-WL vertices are factorizable and hence reduce to computations of lower order and lower loop number.

It is interesting to *classify the possible irreducible diagrams in the 2-body effective action* – those which are both non-factorizable and dressing-irreducible. The possible topologies are independent of the details of the specific field theory. At 1-loop there are no irreducible diagram topologies. At 2-loop (top line of figure 15) there is the “H” diagram on the left

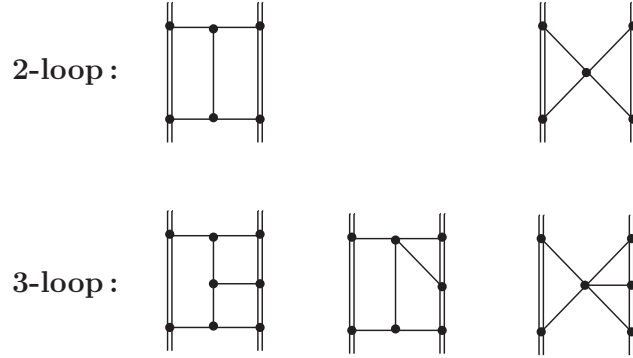


Figure 15: Classification of topologies for irreducible diagrams of the 2-body effective action, both non-factorizable and dressing-irreducible. The top line shows the possibilities at 2-loop, and the bottom line shows the possibilities at 3-loop.

and its degeneration - the “X” diagram where the two cubic bulk vertices degenerate into a quartic vertex. At 3-loop (bottom line of figure 15) there is the topology shown on the left, together with its two possible degenerations. We did not list here the trivial 0-loop (tree-level) diagram shown in figure 1.

3. Dressing the 2-body Post-Newtonian problem

In this section we apply the dressed perturbation theory to the Post-Newtonian (PN) expansion, thereby demonstrating its utility. We start in subsection 3.1 by setting up the problem, establishing the conventions, and displaying the Post-Newtonian effective action and the associated Feynman rules. In subsection 3.2 we explicitly compute the three PN charges both in k -space and in position space up to the order required to reproduce the 2PN results, apart from the stress that is determined to one additional order. In 3.3 we analyze qualitatively the diagrams relevant to the computation of the two-body effective action including a list of all the skeletons required for the computation of 3PN. In subsection 3.4 we compute certain novel 3PN and 4PN diagrams.

3.1 Effective action and Feynman rules

Consider a binary system composed of slowly moving massive objects. Replacing the vicinity of each of these objects by the relativistic point particle coupled to gravity and neglecting the effects of the higher-dimensional tidal terms, leads to the following effective action

$$S = S_{EH} + S_{pp}. \quad (3.1)$$

In PN the gravitational metric field is naturally divided into three fields of Non-Relativistic Gravity (NRG-fields): ϕ the Newtonian potential, A_i the gravito-magnetic vector potential and γ_{ij} a symmetric tensor (with spatial indices) [7]. The field redefinition

$g_{\mu\nu} \rightarrow (\phi, A_i, \gamma_{ij})$ is defined by [6, 7, 8]

$$ds^2 = g_{\mu\nu} dx^\mu dx^\nu = e^{2\phi} (dt - A_i dx^i)^2 - e^{-2\phi/(d-3)} \gamma_{ij} dx^i dx^j , \quad (3.2)$$

where we take the space-time dimension d to be arbitrary and only at the end we shall specialize to 4d. The bulk action is the Einstein-Hilbert action expressed in terms of NRG-fields

$$S_{EH}[g] = \frac{1}{16\pi G} \int R[g] \rightarrow S_{EH}[\gamma, A, \phi] . \quad (3.3)$$

The point particle trajectory is denoted by $\vec{x} = \vec{x}(t)$ and we shall denote by $\vec{v} = \dot{\vec{x}}(t)$ and $\vec{a} = \ddot{\vec{x}}(t)$ its 3-velocity and 3-acceleration, respectively. The point particle action is given by

$$\begin{aligned} S_{pp} &= - \sum_a m_a \int d\tau = - \sum_a m_a \int dt e^\phi \sqrt{(1 - \vec{A} \cdot \vec{v}_a)^2 - e^{-2(d-2)\phi/(d-3)} \gamma_{ij} v_a^i v_a^j} = \\ &= - \sum_a m_a \int dt \sqrt{1 - v_a^2} \\ &\quad - \sum_a m_a \int dt \left(\frac{(d-3) + v_a^2}{(d-3)\sqrt{1 - v_a^2}} \phi - \frac{\vec{A} \cdot \vec{v}_a}{\sqrt{1 - v_a^2}} - \frac{\sigma_{ij} v_a^i v_a^j}{2\sqrt{1 - v_a^2}} + \dots \right) , \end{aligned} \quad (3.4)$$

where the dummy index a runs over all the masses involved in the binary evolution, in the second equality equation (3.2) was applied, the ellipsis denote terms non-linear in the bulk fields (ϕ, A, γ) and we define

$$\sigma_{ij} := \gamma_{ij} - \delta_{ij} . \quad (3.5)$$

The Einstein-Hilbert action is invariant under reparametrizations and should be gauge fixed. Leaving aside the question which gauge would be optimal for this problem, we choose the harmonic gauge in order to facilitate comparison with the literature. Accordingly, we add the following gauge fixing term to the Einstein-Hilbert action

$$S_{GF} = \frac{1}{32\pi G} \int d^d x \sqrt{g} \Gamma^\mu \Gamma^\nu g_{\mu\nu} , \quad (3.6)$$

where $\Gamma^\mu = \Gamma_{\alpha\beta}^\mu g^{\alpha\beta}$.

The Feynman rules for ϕ , A_i and σ_{ij} coupled to the world-line can be read from (3.4) and we list on figure 16 those couplings which are necessary to our discussion. Solid, dashed and wavy lines of the figure are associated with propagators of the instantaneous non-relativistic modes ϕ , A_i and σ_{ij} , respectively. In momentum space these propagators are given by

$$\begin{aligned} \text{————} &= 8\pi G \frac{d-3}{d-2} \delta(t-t') \frac{1}{\mathbf{k}^2} \\ \text{---} &= -16\pi G \delta(t-t') \delta_{ij} \frac{1}{\mathbf{k}^2} \\ \text{~~~~~} &= 32\pi G \delta(t-t') P_{ij,kl} \frac{1}{\mathbf{k}^2} \end{aligned}$$

$$\begin{aligned}
\text{---} \bullet \text{---} &= -m \int dt e^{i\mathbf{k}\cdot\mathbf{x}(t)} \frac{(d-3)+\mathbf{v}^2}{(d-3)\sqrt{1-\mathbf{v}^2}} \\
\text{---} \bullet \text{---} &= m \int dt e^{i\mathbf{k}\cdot\mathbf{x}(t)} \frac{\mathbf{v}_i}{\sqrt{1-\mathbf{v}^2}} \\
\text{---} \bullet \text{---} &= \frac{m}{2} \int dt e^{i\mathbf{k}\cdot\mathbf{x}(t)} \frac{\mathbf{v}_i \mathbf{v}_j}{\sqrt{1-\mathbf{v}^2}}
\end{aligned}$$

Figure 16: Feynman rules obtained from the expansion of (3.4) up to linear order in ϕ , A_i and σ_{ij} . The undetermined wave-numbers flow into the vertex.

with $P_{ij,kl} = \frac{1}{2} \left[\delta_{ik} \delta_{jl} + \delta_{il} \delta_{jk} - \frac{2}{d-3} \delta_{ij} \delta_{kl} \right]$.

The Feynman rules for the bulk vertices are obtained from expansion of the Einstein-Hilbert action (3.3) and the gauge fixing term (3.6). The resulting set of vertices which contribute to the calculations below are presented in figure 17 and figure 18, where we separate vertices which involve time derivatives in figure 18, from the static ones in figure 17.

In addition, one has to impose wave-number⁸ conservation at each bulk vertex by assigning it a delta-function factor, $(2\pi)^{d-1} \delta(\sum_i \mathbf{k}_i)$, where $\sum_i \mathbf{k}_i$ is the total wave-number flow into a given vertex, and one must integrate over each undetermined wave-number \mathbf{k} of the diagram

$$\int_{\mathbf{k}} := \int \frac{d^{d-1}\mathbf{k}}{(2\pi)^{d-1}}. \quad (3.7)$$

Finally, one has to divide by the symmetry factor of the diagram.

3.2 Dressed charges

Given the general theory, it is natural to inquire about the form of the dressed quantities within PN. Accordingly we would like to compute the dressed charges (the dressed propagators are simple and are also discussed below).

Following our discussion at the end of subsection 2.2 on the generalization of the definitions for dressed sub-diagrams to a multi-field field theory we define three dressed charges for the interaction of gravity with a compact point-like object. The ϕ charge is usually

⁸Quantum Mechanically the wave-number k is equivalent to momentum, and this is how k is usually referred to, but in Classical field theory it is not a momentum.

$$\begin{aligned}
& \text{Diagram 1: A vertex with two incoming lines (solid and dashed) labeled } \mathbf{k} \text{ and } \mathbf{q} \text{ respectively, and one outgoing wavy line labeled } lm. \\
& = (16\pi G)^{-1} \frac{d-2}{d-3} (\mathbf{k} \cdot \mathbf{q} \delta_{lm} - 2k_l q_m) \int dt \\
\\
& \text{Diagram 2: A vertex with two incoming lines (dashed and solid) labeled } \mathbf{k}, i \text{ and } \mathbf{q}, j \text{ respectively, and one outgoing solid line.} \\
& = -(8\pi G)^{-1} \frac{d-2}{d-3} (\mathbf{k} \cdot \mathbf{q} \delta_{ij}) \int dt \\
\\
& \text{Diagram 3: A vertex with two incoming lines (dashed and solid) labeled } \mathbf{k}, i \text{ and } \mathbf{q}, j \text{ respectively, and one outgoing wavy line labeled } lm. \\
& = -(32\pi G)^{-1} (\mathbf{q} \cdot \mathbf{k} \delta_{ij} \delta_{lm} - 2\mathbf{q} \cdot \mathbf{k} \delta_{il} \delta_{jm} - (\mathbf{q}_i \mathbf{k}_j - \mathbf{q}_j \mathbf{k}_i) \delta_{lm} \\
& \quad + 2\mathbf{q}_i \mathbf{k}_m \delta_{jl} - 2\mathbf{q}_m \mathbf{k}_l \delta_{ij} + 2\mathbf{q}_m \mathbf{k}_j \delta_{il} - 2\mathbf{q}_l \mathbf{k}_i \delta_{jm} - 2\mathbf{q}_j \mathbf{k}_l \delta_{im}) \int dt
\end{aligned}$$

Figure 17: Static bulk vertices obtained from the expansion of the Hilbert-Einstein action (3.3) and gauge fixing term (3.6) but restricting to time-independent terms. The undetermined wave-numbers flow into the vertex.

referred to as energy, the A charge is the energy current (or alternatively, momentum distribution) and the σ charge is the stress. Together they describe the full energy-momentum tensor (in space-time). In analogy with figure 3 we define the 3 dressed PN charges in figure 19. All the dressed charges describe the changing apparent charge due to non-linear bulk interaction at large, but not infinite, distances.

In PN we have a quadratic retardation vertex for all 3 fields just like in our scalar field example. Since the 3 fields have different tensor characters they cannot mix, and we have exactly 3 dressed propagators each one defined as in figure 7 (bottom). Physically they all correspond to full relativistic propagators, even though A and σ are spatial rather than space-time tensors.

The Feynman diagrams required for the computation of the dressed energy distribution, ρ ,⁹ and the stress, s^{ij} , up to 2PN as well as the dressed momentum distribution, j^i , up to 1.5PN are shown in figure 20, figure 21 and figure 22.¹⁰ The PN order was chosen as the one required for the 2PN effective action, apart for the stress where we chose to compute an additional PN order. All the results below apart from the last term of the dressed stress 2PN were tested and confirmed against the known expression for 2PN effective action. In addition we shall show in the next subsections how to use the dressed charges to calculate diagrams beyond 2PN.

⁹In this section we shall shorten the notation and write ρ rather than ρ_{dr} .

¹⁰Alternatively, one may count PN orders relative to the leading order. With this convention the dressed energy is computed to order +2PN relative to leading, while the dressed momentum and stress are computing to +1PN beyond leading.

$$\begin{aligned}
& \text{Diagram 1: } \partial_t \text{ and } \partial_t \text{ lines meeting at a vertex with a wavy line } lm \text{ attached.} \\
& = (16\pi G)^{-1} \frac{d-2}{d-3} \delta_{lm} \int dt \partial_t^2 \\
& \text{Diagram 2: } \partial_t \text{ line meeting at a vertex with a wavy line } lm \text{ and an outgoing } \partial_t, lm \text{ line.} \\
& = -(8\pi G)^{-1} \frac{(d-2)(d-1)}{(d-3)^2} \delta_{lm} \int dt \partial_t^2 \\
& \text{Diagram 3: } \partial_t \text{ line meeting at a vertex with a wavy line } q, lm \text{ and a dashed line } k, i. \\
& = i(16\pi G)^{-1} \frac{d-2}{d-3} (2\mathbf{q}_i \delta_{im} - \delta_{lm} \mathbf{q}_i) \int dt \partial_t \\
& \text{Diagram 4: } q \text{ line meeting at a vertex with a wavy line } \partial_t, lm \text{ and a dashed line } k, i. \\
& = i(8\pi G)^{-1} \frac{d-2}{d-3} (\mathbf{q}_i \delta_{lm} - \delta_{li} \mathbf{q}_m) \int dt \partial_t \\
& \text{Diagram 5: } \partial_t \text{ and } \partial_t \text{ lines meeting at a vertex with a solid line attached.} \\
& = -(4\pi G)^{-1} \left(\frac{d-2}{d-3}\right)^2 \int dt \partial_t^2 \\
& \text{Diagram 6: } \partial_t \text{ and } \partial_t \text{ lines meeting at a vertex with a dashed line } k, i \text{ attached.} \\
& = -i(8\pi G)^{-1} \frac{d-2}{d-3} \mathbf{q}_i \int dt \partial_t \\
& \text{Diagram 7: } \partial_t \text{ and } \partial_t \text{ lines meeting at a vertex with a crossed line } \partial_t \times \partial_t \text{ attached.} \\
& = (8\pi G)^{-1} \frac{d-2}{d-3} \int dt \partial_t^2
\end{aligned}$$

Figure 18: Time-dependent bulk vertices obtained from the expansion of the Hilbert-Einstein action (3.3) and gauge fixing term (3.6). Time derivative above the propagator indicates the direction on which it acts. The undetermined wave-numbers flow into the vertex.

Given the Feynman rules of the previous subsection, one can write down the expressions for the Feynman integrals. The integrals which are essential for the evaluation of the loop integrals and the Fourier transforms are listed in Appendix A. Note also that since we compute the dressed sources up to a definite order in the PN expansion there is no need to keep the vertices of figure 16 as they are. Instead, one has to expand each such vertex keeping only those powers of “ v ” which contribute to the PN order under consideration.

We proceed to present the results of all the diagrams. We start from the dressed energy distribution. Let us denote

$$\lambda := Gm^2 \frac{\Gamma\left(\frac{3-d}{2}\right) \Gamma\left(\frac{d-1}{2}\right)}{(16\pi)^{\frac{d-4}{2}} \Gamma\left(\frac{d}{2}\right)}, \quad (3.8)$$

$$\begin{aligned}
-\int_{\mathbf{k}} \rho(t, \mathbf{k}) \phi(t, -\mathbf{k}) &:= \text{diagram (a)} \\
\int dt \int_{\mathbf{k}} j^i(t, \mathbf{k}) A_i(t, -\mathbf{k}) &:= \text{diagram (b)} \\
\frac{1}{2} \int dt \int_{\mathbf{k}} s^{ij}(t, \mathbf{k}) \sigma_{ij}(t, -\mathbf{k}) &:= \text{diagram (c)}
\end{aligned}$$

Figure 19: The diagrammatic definition of the dressed charge distributions in PN ρ, j^i and s^{ij} as the one point function for ϕ, A_i and σ_{ij} respectively in the presence of a single source. Retardation vertices are forbidden from the external leg.

$$-\int_{\mathbf{k}} \rho(t, k) \phi(t, -k) = \text{diagram (a)} = \text{diagram (b)} + \text{diagram (c)} + \text{diagram (d)} + \text{diagram (e)} + \text{diagram (f)} + \dots$$

Figure 20: Feynman diagrams which contribute to the dressed energy distribution up to 2PN. Diagram (a) is leading (order 0PN) while the rest are 2PN.

$$\int_{\mathbf{k}} j^i(t, k) A_i(t, -k) = \text{diagram (a)} = \text{diagram (b)} + \text{diagram (c)} + \dots$$

Figure 21: Feynman diagrams which contribute to the dressed momentum distribution up to 1.5PN. Diagram (a) is leading (order 0.5PN) while the rest are +1PN (1.5PN).

then

$$\begin{aligned}
\text{fig.20(a)} &= -m \int dt \frac{(d-3) + v^2}{(d-3)\sqrt{1-v^2}} \phi(t, \vec{x}(t)) \\
&\Rightarrow \delta\rho(t, \vec{x}) = m \left(1 + \frac{d-1}{2(d-3)} v^2 + \frac{3d-5}{8(d-3)} v^4 \right) \delta(\vec{x} - \vec{x}(t)), \\
\delta\rho(t, \vec{k}) &= m \left(1 + \frac{d-1}{2(d-3)} v^2 + \frac{3d-5}{8(d-3)} v^4 \right) \exp(-i\vec{k} \cdot \vec{x}(t)), \quad (3.9)
\end{aligned}$$

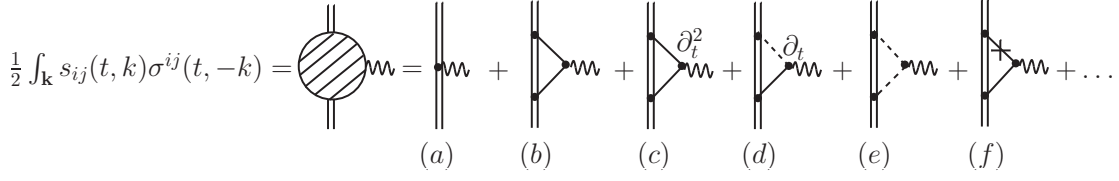


Figure 22: Feynman diagrams which contribute to the dressed stress tensor distribution up to 2PN. Diagrams (a,b) are leading (order 1PN) while the rest are +1PN (2PN).

$$\text{fig.20(b)} = \lambda \frac{(d-2)^2}{2(d-3)} \int dt \vec{v}^2 \int_{\mathbf{k}} e^{-i\vec{k} \cdot \vec{x}(t)} |\vec{k}|^{d-3} \phi(t, -\vec{k}) \quad (3.10)$$

$$\text{fig.20(c)} = \lambda \frac{d-2}{2} \int dt \int_{\mathbf{k}} e^{-i\vec{k} \cdot \vec{x}(t)} |\vec{k}|^{d-5} (\vec{k} \cdot \vec{v})^2 \phi(t, -\vec{k}) \quad (3.11)$$

$$\begin{aligned} \text{fig.20(d)} &= \frac{(16\pi G)^2 m^3}{24} \frac{(d-3)^2}{(d-2)(d-5)} \int dt \int_{\mathbf{k}} e^{-i\vec{k} \cdot \vec{x}(t)} \vec{k}^2 I(|\vec{k}|) \phi(t, -\vec{k}) \\ \Rightarrow \delta\rho(t, \vec{k}) &= -\frac{(16\pi G)^2 m^3}{24} \frac{(d-3)^2}{(d-2)(d-5)} e^{-i\vec{k} \cdot \vec{x}(t)} \vec{k}^2 I(|\vec{k}|), \end{aligned} \quad (3.12)$$

with

$$I(|\vec{k}|) = \sqrt{\pi} \frac{\Gamma(4-d)}{(4\pi)^{d-1}} \frac{\Gamma(d/2-3/2)^2 \Gamma(d-3)}{\Gamma(d/2-1) \Gamma(3d/2-9/2)} \left(\frac{\vec{k}^2}{2} \right)^{d-4}. \quad (3.13)$$

Apparently, the above expression possesses a pole when $d = 4$, and thus one needs to introduce a counter-term which inevitably leads to a logarithmic behavior of the dressed energy distribution with scale. Yet this pole unphysical. Indeed, applying a Fourier transform to equation (3.12) yields

$$\delta\rho(t, \vec{r}) = (8\pi G)^2 \left(\frac{m}{\Omega_{d-2}} \right)^3 \frac{(d-3)}{(d-2)(d-5)} |\vec{r}|^{7-3d}, \quad (3.14)$$

where

$$\Omega_{d-2} = \frac{2\pi^{\frac{d-1}{2}}}{\Gamma(\frac{d-1}{2})}, \quad \vec{r} = \vec{x} - \vec{x}(t). \quad (3.15)$$

and this expression is regular for $d = 4$.

Alternatively, one could stay within the wave-number space (k -space) by introducing the following counter-term

$$\text{c.t.} = -\frac{G^2 m^3}{6(d-4)} \int dt \int_{\mathbf{k}} e^{-i\vec{k} \cdot \vec{x}(t)} \vec{k}^2 \phi(t, -\vec{k}) = \frac{G^2 m^3}{6(d-4)} \int dt \square \phi(t, \vec{x}(t)). \quad (3.16)$$

However, as explained in [5] such a term can be removed from the Lagrangian by an appropriate field redefinition as it is proportional to the leading order equation of motion for the NRG field ϕ and hence it is a redundant term.¹¹

¹¹In quantum field theory such an objects is called a redundant *operator* referring to its action on the Hilbert space of states. In the classical theory it is not an operator and calling it a *term* is more appropriate.

The contribution to the energy distribution of the diagrams which contain time derivatives is given by

$$\begin{aligned}
\text{fig.20(e)} &= -\frac{\lambda}{8} \int dt \int_{\mathbf{k}} e^{-i\vec{k} \cdot \vec{x}(t)} \\
&\quad \times |\vec{k}|^{d-5} \left[\vec{k}^2 \vec{v}^2 - (3d-5)(\vec{k} \cdot \vec{v})^2 - 4(d-2)(i\vec{k} \cdot \vec{a}) \right] \phi(t, -\vec{k}) \\
\text{fig.20(f)} &= -\frac{d-2}{2} \lambda \int dt \int_{\mathbf{k}} e^{-i\vec{k} \cdot \vec{x}(t)} |\vec{k}|^{d-5} \left[i\vec{k} \cdot \vec{a} + 2(\vec{k} \cdot \vec{v})^2 \right] \phi(t, -\vec{k}) \quad (3.17)
\end{aligned}$$

Combining altogether we get up to 2PN

$$\begin{aligned}
\rho(t, \vec{k}) e^{i\vec{k} \cdot \vec{x}(t)} &= m \left(1 + \frac{d-1}{2(d-3)} v^2 + \frac{3d-5}{8(d-3)} v^4 \right) - \frac{(16\pi G)^2 m^3}{24} \frac{(d-3)^2}{(d-2)(d-5)} \vec{k}^2 I(|\vec{k}|) \\
&\quad - \frac{4d^2 - 17d + 19}{8(d-3)} \lambda |\vec{k}|^{d-3} v^2 + \frac{d-3}{8} \lambda |\vec{k}|^{d-5} (\vec{k} \cdot \vec{v})^2. \quad (3.18)
\end{aligned}$$

where the exponential on the left hand side really belongs on the right hand side and was moved from there to achieve a “cleaner” form. Transforming back to coordinate space yields

$$\begin{aligned}
\rho(t, \vec{r}) &= m \left(1 + \frac{d-1}{2(d-3)} v^2 + \frac{3d-5}{8(d-3)} v^4 \right) \delta(\vec{r}) \\
&\quad + 8\pi G \left(\frac{m}{\Omega_{d-2}} \right)^2 \left[(\vec{v} \cdot \hat{r})^2 - 2 \frac{d-2}{d-3} v^2 \right] |\vec{r}|^{4-2d} \\
&\quad + (8\pi G)^2 \left(\frac{m}{\Omega_{d-2}} \right)^3 \frac{(d-3)}{(d-2)(d-5)} |\vec{r}|^{7-3d}. \quad (3.19)
\end{aligned}$$

The results for the dressed momentum distribution up to 1.5PN are

$$\begin{aligned}
\text{fig.21(a)} &= \int dt \frac{m v^i}{\sqrt{1-v^2}} A_i(t, \vec{x}(t)) \\
&\Rightarrow \delta j^i(t, \vec{x}) = m v^i \left(1 + \frac{1}{2} v^2 \right) \delta(\vec{x} - \vec{x}(t)), \\
&\quad \delta j^i(t, \vec{k}) = m v^i \left(1 + \frac{1}{2} v^2 \right) \exp(-i\vec{k} \cdot \vec{x}(t)), \\
\text{fig.21(b)} &= -\lambda \frac{d-2}{2} \int dt \int_{\mathbf{k}} e^{-i\vec{k} \cdot \vec{x}(t)} |\vec{k}|^{d-3} \vec{v} \cdot \vec{A}(t, -\vec{k}) \\
\text{fig.21(c)} &= \lambda \frac{d-3}{8(d-2)} \int dt \int_{\mathbf{k}} e^{-i\vec{k} \cdot \vec{x}(t)} |\vec{k}|^{d-5} (\vec{k}^2 v_i + (d-3)(\vec{k} \cdot \vec{v}) k_i) A^i(t, -\vec{k}) \quad (3.20)
\end{aligned}$$

Altogether we obtain up to 1.5PN

$$\begin{aligned}
j^i(t, \vec{k}) e^{i\vec{k} \cdot \vec{x}(t)} &= m v^i \left(1 + \frac{1}{2} v^2 \right) - \frac{4d^2 - 17d + 19}{8(d-2)} \lambda |\vec{k}|^{d-3} v^i \\
&\quad + \frac{(d-3)^2}{8(d-2)} \lambda |\vec{k}|^{d-5} (\vec{k} \cdot \vec{v}) k^i. \quad (3.21)
\end{aligned}$$

In coordinate space the dressed momentum distribution is

$$j^i(t, \vec{r}) = m v^i \left(1 + \frac{1}{2} v^2 \right) \delta(\vec{r}) + 8\pi G \left(\frac{m}{\Omega_{d-2}} \right)^2 \left[\frac{d-3}{d-2} (\vec{v} \cdot \hat{r}) \hat{r}^i - 2 v^i \right] |\vec{r}|^{4-2d}. \quad (3.22)$$

Finally, the results for the dressed stress charge up to 2PN are given by

$$\begin{aligned} \text{fig.22(a)} &= \frac{m}{2} \int dt \frac{v^i v^j}{\sqrt{1-v^2}} \sigma_{ij}(t, \vec{x}) \\ &\Rightarrow \delta s^{ij}(t, \vec{x}) = m v^i v^j \left(1 + \frac{1}{2} v^2 \right) \delta(\vec{x} - \vec{x}(t)), \\ \delta s^{ij}(t, \vec{k}) &= m v^i v^j \left(1 + \frac{1}{2} v^2 \right) \exp(-i\vec{k} \cdot \vec{x}(t)), \end{aligned} \quad (3.23)$$

$$\text{fig.22(b)} = \lambda \frac{(d-3)^2}{16(d-2)} \int dt \left(1 + \frac{d-1}{d-3} v^2 \right) \int_{\mathbf{k}} e^{-i\vec{k} \cdot \vec{x}(t)} |\vec{k}|^{d-5} \left[k_i k_j - \vec{k}^2 \delta_{ij} \right] \sigma^{ij}(t, -\vec{k}) \quad (3.24)$$

$$\begin{aligned} \text{fig.22(c)} &= \lambda \frac{d-3}{32(d-2)} \int dt \int_{\mathbf{k}} e^{-i\vec{k} \cdot \vec{x}(t)} |\vec{k}|^{d-5} \\ &\times \left[\frac{(3d-5)^2}{d-3} (\vec{k} \cdot \vec{v})^2 + \vec{k}^2 \vec{v}^2 + \frac{8(d-1)(d-2)}{d-3} i\vec{k} \cdot \vec{a} \right] \delta_{ij} \sigma^{ij}(t, -\vec{k}) \end{aligned} \quad (3.25)$$

$$\text{fig.22(d)} = \lambda \frac{d-2}{2} \int dt \int_{\mathbf{k}} e^{-i\vec{k} \cdot \vec{x}(t)} |\vec{k}|^{d-5} \left[\frac{1}{2} (\vec{k} \cdot \vec{v})^2 \delta_{ij} + (i\vec{k} \cdot \vec{a}) \delta_{ij} - i k_i a_j \right] \sigma^{ij}(t, -\vec{k}) \quad (3.26)$$

$$\text{fig.22(e)} = \frac{\lambda}{8} \int dt \int_{\mathbf{k}} e^{-i\vec{k} \cdot \vec{x}(t)} |\vec{k}|^{d-5} \left[(d-3)(\vec{k}^2 \vec{v}^2 \delta_{ij} - \vec{v}^2 k_i k_j) - 2(d-2) \vec{k}^2 v_i v_j \right] \sigma^{ij}(t, -\vec{k}) \quad (3.27)$$

$$\begin{aligned} \text{fig.22(f)} &= -\frac{\lambda}{4} \frac{d-3}{d-2} \int dt \int_{\mathbf{k}} e^{-i\vec{k} \cdot \vec{x}(t)} |\vec{k}|^{d-5} \\ &\times \left[\frac{d-2}{8} \vec{k}^2 \vec{v}^2 - \frac{(d-3)(d-4)}{8} (\vec{k} \cdot \vec{v})^2 - \frac{d^2-7d+11}{4} (i\vec{k} \cdot \vec{a}) \right] \delta_{ij} \sigma^{ij}(t, -\vec{k}) \\ &- \frac{\lambda}{4} \frac{d-3}{d-2} \int dt \int_{\mathbf{k}} e^{-i\vec{k} \cdot \vec{x}(t)} |\vec{k}|^{d-5} \\ &\times \left[-\frac{d-3}{8} \vec{v}^2 k_i k_j + \frac{(d-3)(d-5)}{8} (\vec{k} \cdot \vec{v})^2 k_i k_j - \frac{1}{4} \vec{k}^2 v_i v_j \right] \sigma^{ij} \\ &- \frac{\lambda}{4} \frac{d-3}{d-2} \int dt \int_{\mathbf{k}} e^{-i\vec{k} \cdot \vec{x}(t)} |\vec{k}|^{d-5} \left[-\frac{i k_i a_j}{2} + \frac{(d-3)(d-5)}{4} (\vec{k} \cdot \vec{a}) i \hat{k}_i \hat{k}_j \right] \sigma^{ij} \end{aligned} \quad (3.28)$$

As a result, the dressed stress charge up to 2PN is given by

$$\begin{aligned}
s^{ij}(t, \vec{k}) e^{i\vec{k}\cdot\vec{x}(t)} &= m v^i v^j \left(1 + \frac{1}{2}v^2\right) - \frac{4d^2 - 17d + 19}{4(d-2)} \left(ik^{(i}a^{j)} + \frac{\vec{k}^2}{2}v^i v^j\right) |\vec{k}|^{d-5}\lambda \\
&+ \frac{(d-3)^2}{8(d-2)} \left(1 - \frac{v^2}{2} - \frac{d-5}{2}(\vec{v}\cdot\hat{k})^2 - (d-5)\frac{i\vec{a}\cdot\vec{k}}{\vec{k}^2}\right) k^i k^j |\vec{k}|^{d-5}\lambda \\
&+ \left[\frac{(d-1)(d^2+8d-21)}{16(d-2)}(\vec{k}\cdot\vec{v})^2 + \frac{d^3+2d^2-12d+7}{8(d-2)}i\vec{a}\cdot\vec{k}\right] |\vec{k}|^{d-5}\lambda\delta^{ij} \\
&- \frac{(d-3)^2}{8(d-2)} \left(1 - \frac{v^2}{2}\right) |\vec{k}|^{d-3}\lambda\delta^{ij}, \tag{3.29}
\end{aligned}$$

where (ij) denotes symmetrization with respect to indices i and j with factor $1/2$ included. In the coordinate space we obtain

$$\begin{aligned}
s^{ij}(t, \vec{r}) &= m v^i v^j \left(1 + \frac{1}{2}v^2\right) \delta(\vec{r}) - \frac{(3d-5)}{(d-2)(d-3)} f(r) \vec{r}^{(i}a^{j)} - 2f(r) v^i v^j \\
&- \frac{d^2+10d-15}{4(d-2)(d-3)} f(r) (v^2 - 2(d-2)(\vec{v}\cdot\hat{r})^2) \delta^{ij} \\
&- \frac{d-3}{d-2} f(r) \left((d-1)(\vec{v}\cdot\hat{r})^2 \hat{r}^i \hat{r}^j - 2(\vec{v}\cdot\hat{r}) v^i \hat{r}^j + \frac{1}{2} \left(1 - \frac{v^2}{2}\right) \delta^{ij} - \hat{r}^i \hat{r}^j + (\vec{a}\cdot\vec{r}) \hat{r}^i \hat{r}^j \right) \\
&+ \frac{d^2+5d-8}{2(d-2)(d-3)} f(r) (\vec{a}\cdot\vec{r}) \delta^{ij}. \tag{3.30}
\end{aligned}$$

with

$$f(r) = \frac{8\pi G}{|\vec{r}|^{2d-4}} \left(\frac{m}{\Omega_{d-2}} \right)^2. \tag{3.31}$$

3.3 Skeletons for 2PN and 3PN

We shall now demonstrate how all the bare diagrams of the two-body effective action up to 2PN, order by order transform into their dressed form, including their corresponding skeletons.

At 0PN (Newtonian order) a single diagram (figure 1) contributes representing the interaction of two tree-level masses.

At 1PN (Einstein-Infeld-Hoffmann Lagrangian) the four diagrams shown in figure 23 contribute. The first is a v^2 component of the mass vertex and can be considered to be a trivial dressing of the energy. The second is the tree-level interaction of two currents. The third represents a propagator dressing (retardation) of the Newtonian potential. Finally the fourth is due to a non-linear world-line vertex which accounts for the gravitating nature of potential energy. Altogether none is irreducible with a topology other than Newtonian. We note that the last diagram is of order $\mathcal{O}(G^2 m^3 v^0)$ where m represents a typical mass and v a typical velocity while all the previous diagrams are of order $\mathcal{O}(Gm^2 v^2)$.

At 2PN Gilmore and Ross [8] found 21 diagrams. We shall see that many can be interpreted to represent dressing effects while only one is both non-factorizable and dressing-irreducible. Indeed [8] find its computation to be the core or essential computation at this order.

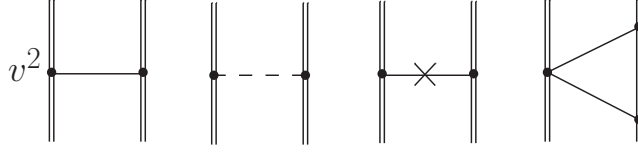


Figure 23: The four diagrams which contribute to the two-body effective action at 1PN – The Einstein-Infeld-Hoffmann Lagrangian.

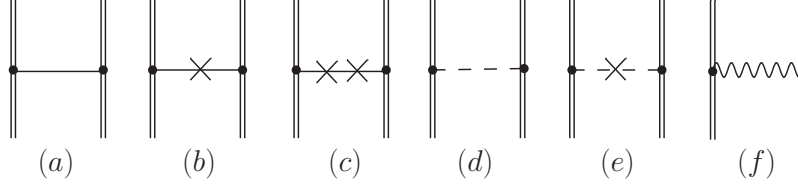


Figure 24: 2PN Diagrams contributing at order $\mathcal{O}(Gm^2v^4)$ (following [8]).

The six diagrams (a-f) shown in figure 24 contribute at order $\mathcal{O}(Gm^2v^4)$. Diagrams (b,c,e) represent propagator dressing to diagrams from lower orders, while the rest involve only tree-level v -dependent vertices.

At order $\mathcal{O}(G^2m^3v^2)$ there are 10 diagrams shown in figure 25. Diagrams (a,b,c) are V-shaped and as such factorizable and at least one factor is the Newtonian potential. Diagrams (d-j) are Y-shaped and as such are dressing-reducible. Four diagrams (d,f,g,i) represent mass dressing, the two (e,h) represent current dressing, while finally (j) can be thought to represent stress dressing.

At order $\mathcal{O}(G^3m^4v^0)$ there are 5 diagrams. Both (a) and (c) factorize into 3 Newtonian-potential factors. Diagrams (b) represents a mass dressing (the circled piece) while (e) includes two σ dressing sub-diagrams. Finally diagram (d) is the one and only truly irreducible diagram at 2PN. Actually for some yet-unexplained reason the computation reduces after several steps to a square of the master one-loop integral. We speculate that this is special to the GR action (and is not generic to classical field theories) and in particular to the gauge symmetry which may relate this diagram to other diagrams at 2PN.

As a result of this analysis we can extract all the non-factorizable skeletons up to 2PN. These are listed in figure 27, where the skeletons are labeled according to the PN order in which they first appear. By evaluating the dressed diagrams we successfully tested our expressions for the dressed charges from the previous subsection against the known expressions for the effective action.

3PN. As a step towards the determination of 3PN we extend the list of skeletons up to that order using the classification of possible topologies in figure 15 and some knowledge on the Feynman rules of PN. Taken together with the evaluation of the dressed vertices (partially obtained in the last subsection) this list of skeletons leads the way to a determination of the 3PN part of the 2-body effective action. We note that the 3-loop topologies of figure 15 are *not* realized at 3PN. The reason is the absence in PN of certain bulk vertices

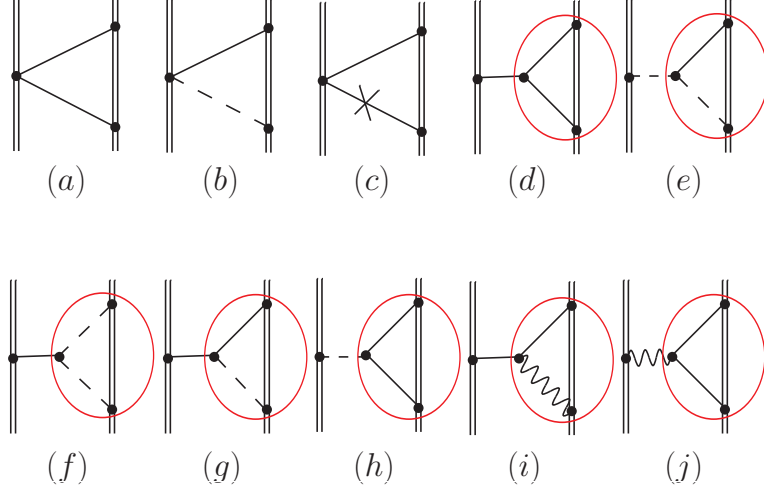


Figure 25: 2PN Diagrams contributing at order $\mathcal{O}(G^2 m^3 v^2)$ (following [8]).

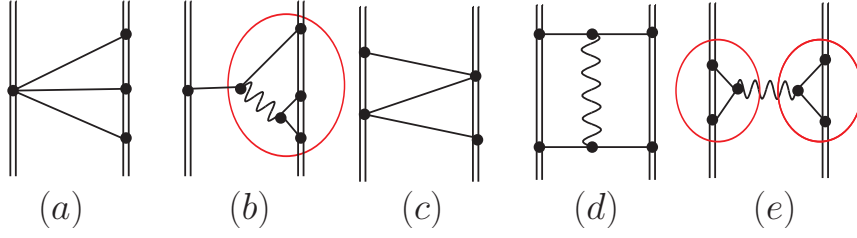


Figure 26: 2PN Diagrams contributing at order $\mathcal{O}(G^3 m^4 v^0)$ (following [8]).

such as ϕ^3 .

3.4 Computing beyond 2PN

In this subsection we explicitly demonstrate the economizing ability of proposed approach in several cases

- A certain economization during 2PN calculation.
- Using the dressed energy distribution computed above in subsection 3.2 to calculate terms of the Newtonian interaction type of order 3PN and 4PN.
- Similarly, using the computed dressed momentum distributions we calculate a current-current interaction term of order 3PN.
- Finally, we use our highest order results for the dressed stress in order to compute 3PN terms by attaching the external σ leg to the second compact object.

An application at 2PN. The first non-trivial example appears during the computation of the 2-body effective Lagrangian at order 2PN. Indeed the dressed stress sub-diagram

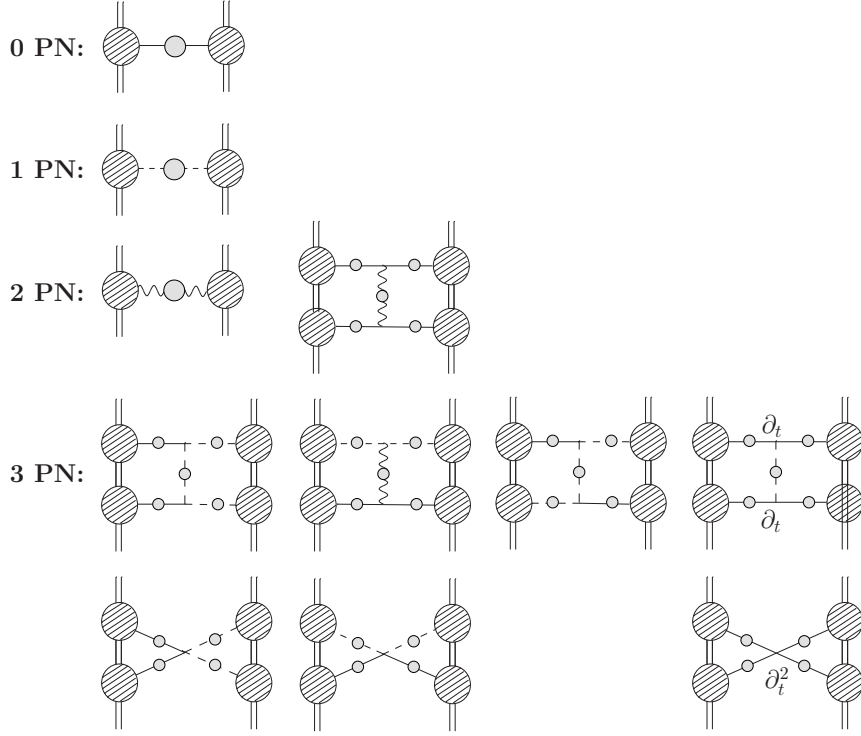


Figure 27: A listing of all non-factorizable skeletons appearing in the dressed Post-Newtonian perturbation theory up to 3PN, listed by the PN order at which they first appear.

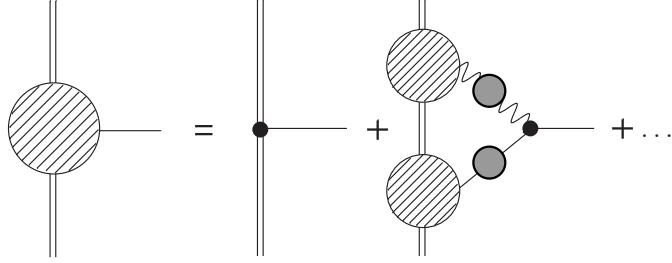


Figure 28: The diagrammatic representation of the recursive integral equation satisfied by the dressed energy.

in figure 22(b) appears twice at 2PN – both at figure 25(j) and at figure 26(b), and of course it is enough to evaluate it once. Another point of view is to obtain both dressed energies corresponding to figures 20(c,d) from the recursive relation shown in figure 28 after substituting in the leading contribution to the dressed stress from figures 22(a,b).

Proceeding **beyond 2PN** we shall now compute certain 3PN and 4PN terms in the 2-body effective action building on the results of the previous section. Pictorially these terms are shown on figure 29, where the bubbles represent the dressed charges, and we explicitly indicate on each bubble which piece of the dressed charge is essential to the computation.

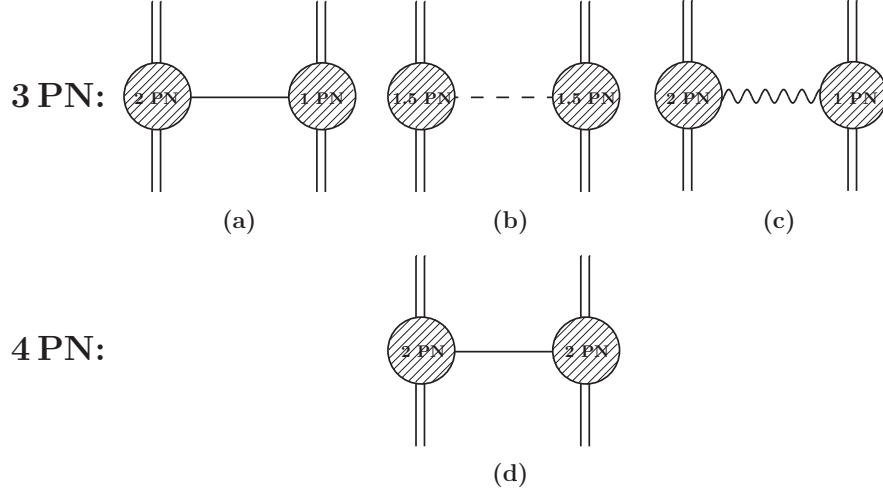


Figure 29: The diagrammatic representation of terms beyond 2PN in the 2-body effective action: (a) a 3PN ρ - ρ term, (b) a 3PN j - j term, (c) a 3PN s - s term and finally (d) a 4PN ρ - ρ term.

Building on the Feynman rules of the previous section, we obtain

$$\text{fig.29(a, d)} = 8\pi G \frac{d-3}{d-2} \int dt \int_{\mathbf{k}} \frac{\rho_2(t, -\vec{k}) \rho_1(t, \vec{k})}{\vec{k}^2}, \quad (3.32)$$

$$\text{fig.29(b)} = -16\pi G \int dt \int_{\mathbf{k}} \frac{\vec{j}_2(t, -\vec{k}) \cdot \vec{j}_1(t, \vec{k})}{\vec{k}^2}, \quad (3.33)$$

$$\text{fig.29(c)} = 8\pi G \int dt \int_{\mathbf{k}} \frac{s_2^{ij}(t, -\vec{k}) P_{ij,kl} s_1^{kl}(t, \vec{k})}{\vec{k}^2}, \quad (3.34)$$

The 3PN j - j and s - s terms. Substituting (3.21),(3.29) and $d = 4$ into (3.33),(3.34) yields

$$\begin{aligned} \text{fig.29(b)} = & - \int dt \frac{Gm_1 m_2}{r} (\vec{v}_1 \cdot \vec{v}_2) v_1^2 v_2^2 \\ & - \int dt \frac{Gm_1 m_2}{2r} \left(\frac{Gm_2}{r} v_1^2 + \frac{Gm_1}{r} v_2^2 \right) [7(\vec{v}_1 \cdot \vec{v}_2) + (\vec{v}_1 \cdot \hat{r})(\vec{v}_2 \cdot \hat{r})] \\ & + \frac{7\pi^2}{32} \int dt \frac{G^3 m_1^2 m_2^2}{r^3} (\vec{v}_1 \cdot \vec{v}_2 - 3(\vec{v}_1 \cdot \hat{r})(\vec{v}_2 \cdot \hat{r})), \end{aligned} \quad (3.35)$$

$$\begin{aligned}
\text{fig.29(c)} = & \int dt \frac{Gm_1 m_2}{r} [(v_1 \cdot v_2)^2 - v_1^2 v_2^2] v_1^2 + \int dt \frac{G^2 m_1^2 m_2}{r^2} \left[\frac{1}{2} (\vec{v}_1 \cdot \vec{v}_2)^2 + \frac{203}{12} v_2^2 v_1^2 \right] \\
& + \int dt \frac{G^2 m_1^2 m_2}{r^2} \left[-\frac{22}{3} (\vec{v}_2 \cdot \vec{r})(\vec{a}_1 \cdot \vec{v}_2) - \frac{121}{4} v_2^2 (\vec{a}_1 \cdot \vec{r}) - \frac{1}{6} (\vec{a}_1 \cdot \vec{r})(\vec{v}_2 \cdot \vec{r})^2 \right] \\
& - \int dt \frac{G^2 m_1^2 m_2}{r^2} \left[\frac{245}{6} v_2^2 (\vec{v}_1 \cdot \vec{r})^2 + \frac{1}{4} v_1^2 (\vec{v}_2 \cdot \vec{r})^2 + \frac{1}{3} (\vec{v}_1 \cdot \vec{r})^2 (\vec{v}_2 \cdot \vec{r})^2 + \frac{1}{12} (\vec{v}_1 \cdot \vec{v}_2)^2 \right] \\
& + \frac{1}{3} \int dt \frac{G^2 m_1^2 m_2}{r^2} [(\vec{v}_1 \cdot \vec{v}_2)(\vec{v}_1 \cdot \vec{r})(\vec{v}_2 \cdot \vec{r})] + (1 \leftrightarrow 2) .
\end{aligned} \tag{3.36}$$

where $\vec{r}(t) = \vec{x}_2(t) - \vec{x}_1(t)$ denotes the radius vector between the particles, and we have neglected the contact term proportional to $\delta(\vec{r})$ since in CLEFT particles are widely separated from each other.

The ρ - ρ terms. Let us now evaluate figure 29(b). First note, that since equation (3.12) contains a simple pole in $d = 4$ one concludes that the integrand of (3.32) possesses a double pole, and thus in contrast to the previous case (3.14) a Fourier transform will not lead to a regular expression.

Therefore, we expand equation (3.12) around $d = 4$

$$\begin{aligned}
\text{fig.20(d)} = & G^2 m_r^3 L^{-\epsilon} \int dt \int_{\mathbf{k}} e^{-i\vec{k} \cdot \vec{x}(t)} \vec{k}^2 \phi(t, -\vec{k}) \\
& \times \left[-\frac{1}{6\epsilon} + \frac{1}{12} \left(-1 + 2\gamma - 2\ln(8\pi^2) + 2\ln(\vec{k}^2 L^2) \right) + \mathcal{O}(\epsilon) \right] ,
\end{aligned} \tag{3.37}$$

where γ is Euler's constant and motivated by the QFT renormalization approach we introduced an arbitrary length scale L and the following definitions¹²

$$\epsilon = 4 - d , \quad Gm = Gm_r L^{-\epsilon} . \tag{3.38}$$

In order to eliminate the divergence as $\epsilon \rightarrow 0$, we add the following counter-term to the effective action

$$\text{c.t.} = c \int dt \Delta\phi(t, \vec{x}(t)) = -c \int dt \int_{\mathbf{k}} e^{-i\vec{k} \cdot \vec{x}(t)} \vec{k}^2 \phi(t, -\vec{k}) , \tag{3.39}$$

where

$$c = L^{-\epsilon} \left(c_r - \frac{G^2 m_r^3}{6\epsilon} \right) . \tag{3.40}$$

¹²Index "r" stands for "renormalized", though in the current work we will not encounter divergences associated with non-trivial RG flow of the mass.

Since the renormalization scale L introduced above is arbitrary, we must have

$$\begin{aligned}
0 &= L \frac{dm}{dL} = L^{-\epsilon} \left(-\epsilon m_r + L \frac{dm_r}{dL} \right) \\
&\Rightarrow L \frac{dm_r}{dL} = \epsilon m_r \quad , \\
0 &= L \frac{dc}{dL} = -\epsilon L^{-\epsilon} \left(c_r - \frac{G^2 m_r^3}{6\epsilon} \right) + L^{-\epsilon} \left(L \frac{dc_r}{dL} - \frac{G^2 m_r^2}{2\epsilon} L \frac{dm_r}{dL} \right) \\
&\Rightarrow L \frac{dc_r}{dL} = \epsilon c_r + \frac{G^2 m_r^3}{3} \quad .
\end{aligned} \tag{3.41}$$

Apparently, the theory exhibits a non-trivial RG flow. But as argued in [5] this scaling is not physical in nature and can be removed by a suitable field redefinition which is tantamount to a coordinate transformation. Indeed, combining (3.37) with (3.39) yields

$$\delta\rho(t, \vec{k}) = \left[c_r - \frac{G^2 m_r^3}{12} \left(-1 + 2\gamma - 2\ln(8\pi^2) + 2\ln(\vec{k}^2 L^2) \right) \right] e^{-i\vec{k} \cdot \vec{x}(t)} \vec{k}^2 \quad . \tag{3.42}$$

In coordinate space this expression is given by

$$\delta\rho(t, \vec{r}) = \left[c_r - \frac{G^2 m_r^3}{12} \left(-1 + 2\gamma - 2\ln(8\pi^2) \right) \right] \delta(\vec{r}) - \frac{1}{2\pi} \frac{G^2 m_r^3}{r^5} \quad , \tag{3.43}$$

where $\vec{r} = \vec{x} - \vec{x}(t)$ and the relation

$$\ln \vec{k}^2 = \lim_{\alpha \rightarrow 0} \frac{d}{d\alpha} (k^2)^\alpha \tag{3.44}$$

was used in order to apply the Fourier transform formulas of Appendix A.

However, the contact term in the above expression for $\delta\rho$ can be eliminated by the following field redefinition

$$\phi \rightarrow \phi + 4\pi G \left[c_r - \frac{G^2 m_r^3}{12} \left(-1 + 2\gamma - 2\ln(8\pi^2) \right) \right] \delta(\vec{r}) \quad . \tag{3.45}$$

As a result, we reproduced equation (3.14) for $d = 4$ and also obtained the regularized expression for $\rho(t, \vec{k})$ in four dimensions¹³

$$\rho(t, \vec{k}) e^{i\vec{k} \cdot \vec{x}(t)} = m \left(1 + \frac{3}{2} v^2 + \frac{7}{8} v^4 \right) + \frac{\pi}{8} G m^2 |\vec{k}| \left(15v^2 - (\hat{k} \cdot \vec{v})^2 \right) - \frac{G^2 m^3}{6} \vec{k}^2 \ln(\vec{k}^2 L^2) \quad . \tag{3.46}$$

A comment should be made regarding the field redefinition (3.45). Obviously, such a shift introduces an extra term to the world-line action as a side effect. This term is proportional to the second derivative of the NRG field ϕ with respect to time. However, it can be removed by including additional counter-term given by

$$\text{c.t.} = \tilde{c} \int dt \frac{\partial^2 \phi}{\partial t^2}(t, \vec{x}(t)) \quad . \tag{3.47}$$

¹³We omit index "r" to avoid abuse of notation.

We will not elaborate the details of this elimination as they are irrelevant to the computation of the 4PN term.

Substituting (3.46) into (3.32) leads to

$$\begin{aligned} \text{fig.29(a)} = & \frac{21}{16} \int dt \frac{G m_1 m_2}{r} v_1^2 v_2^4 \\ & + \frac{3}{2} \int dt \frac{G^2 m_2^2 m_1}{r^2} v_1^2 \left[\frac{7}{2} v_2^2 + \frac{(\vec{v}_2 \cdot \hat{r})^2}{2} + \frac{1}{3} \frac{G m_2}{r} \right] + (1 \leftrightarrow 2) , \end{aligned} \quad (3.48)$$

and

$$\begin{aligned} \text{fig.29(d)} = & \frac{49}{64} \int dt \frac{G m_1 m_2}{r} v_1^4 v_2^4 + \frac{7}{8} \int dt \frac{G^2 m_2^2 m_1}{r^2} v_1^4 \left[\frac{7}{2} v_2^2 + \frac{(\vec{v}_2 \cdot \hat{r})^2}{2} + \frac{1}{3} \frac{G m_2}{r} \right] \\ & + \frac{7}{8} \int dt \frac{G^2 m_1^2 m_2}{r^2} v_2^4 \left[\frac{7}{2} v_1^2 + \frac{(\vec{v}_1 \cdot \hat{r})^2}{2} + \frac{1}{3} \frac{G m_1}{r} \right] \\ & + \frac{\pi^2}{64} \int dt \frac{G^3 m_1^2 m_2^2}{r^3} [(\vec{v}_1 \cdot \vec{v}_2)^2 - \frac{59}{2} v_1^2 v_2^2 + \frac{87}{2} v_1^2 (\vec{v}_2 \cdot \hat{r})^2 + \frac{87}{2} v_2^2 (\vec{v}_1 \cdot \hat{r})^2 \\ & \quad + \frac{15}{2} (\vec{v}_2 \cdot \hat{r})^2 (\vec{v}_1 \cdot \hat{r})^2 - 6 (\vec{v}_2 \cdot \hat{r}) (\vec{v}_1 \cdot \hat{r}) (\vec{v}_1 \cdot \vec{v}_2)] \\ & + \frac{1}{3} \int dt \frac{G^4 m_1^2 m_2^3}{r^4} \left[v_1^2 \left(\frac{23}{2} - 8\gamma - 8 \ln(r/L) \right) + (\vec{v}_1 \cdot \hat{r})^2 \left(-\frac{3}{2} + 2\gamma + 2 \ln(r/L) \right) \right] \\ & + \frac{1}{3} \int dt \frac{G^4 m_1^3 m_2^2}{r^4} \left[v_2^2 \left(\frac{23}{2} - 8\gamma - 8 \ln(r/L) \right) + (\vec{v}_2 \cdot \hat{r})^2 \left(-\frac{3}{2} + 2\gamma + 2 \ln(r/L) \right) \right] \\ & - \frac{4}{9} \int dt \frac{G^5 m_1^3 m_2^3}{r^5} [3 - 2\gamma - 2 \ln(r/L)] . \end{aligned} \quad (3.49)$$

To derive this expression we first applied (3.44) and then used transform Fourier master integrals of Appendix A. Appearance of an arbitrary renormalization scale L in the above expression should not be taken as a strong evidence for a non-trivial RG flow, since if other terms in the full 4PN potential are considered then cancelation of logs might occur.

Acknowledgements

It is a pleasure to thank Gabriele Veneziano for his lectures series “Transplanckian scattering” (Institute for Advanced Studies at Jerusalem, March 2009, based in part on [35, 36]) which catalyzed the beginning of this work; Ofer Aharony, Ira Rothstein and Gerhard Schäfer for very useful comments on the manuscript; and finally the organizers of the following meetings where part of this work was performed: “The fifth Crete regional meeting in String Theory” (Crete, June-July 09), and “Gravity - New perspectives from strings and higher dimensions” (Benasque, July 09). In addition MS thanks the Perimeter Institute for their kind hospitality during the completion of this work.

This research is supported by The Israel Science Foundation grant no 607/05, by the German Israel Cooperation Project grant DIP H.52, and the Einstein Center at the Hebrew University.

A. Master integrals

In this appendix we present master integrals which we found useful during the calculations presented in the text. We start with

$$J = \int \frac{d^d \mathbf{q}}{(2\pi)^d} \frac{1}{(\mathbf{q}^2)^\alpha [(\mathbf{q} - \mathbf{k})^2]^\beta} = \frac{(\mathbf{k}^2)^{d/2-\alpha-\beta}}{(4\pi)^{d/2}} \frac{\Gamma(\alpha + \beta - d/2)}{\Gamma(\alpha)\Gamma(\beta)} \frac{\Gamma(d/2 - \alpha)\Gamma(d/2 - \beta)}{\Gamma(d - \alpha - \beta)} \quad (\text{A.1})$$

$$J_i = \int \frac{d^d \mathbf{q}}{(2\pi)^d} \frac{q_i}{(\mathbf{q}^2)^\alpha [(\mathbf{q} - \mathbf{k})^2]^\beta} = \frac{d/2 - \alpha}{d - \alpha - \beta} J k_i \quad (\text{A.2})$$

$$\begin{aligned} J_{ij} &= \int \frac{d^d \mathbf{q}}{(2\pi)^d} \frac{q_i q_j}{(\mathbf{q}^2)^\alpha [(\mathbf{q} - \mathbf{k})^2]^\beta} \\ &= \frac{1}{(4\pi)^{d/2}} \frac{\Gamma(\alpha + \beta - d/2 - 1)}{\Gamma(\alpha)\Gamma(\beta)} \frac{\Gamma(d/2 - \alpha + 1)\Gamma(d/2 - \beta)}{\Gamma(d - \alpha - \beta + 2)} \\ &\quad \times \left[(d/2 - \alpha + 1)(\alpha + \beta - d/2 - 1)k_i k_j + (d/2 - \beta) \frac{\mathbf{k}^2}{2} \delta_{ij} \right] (\mathbf{k}^2)^{d/2-\alpha-\beta} \end{aligned} \quad (\text{A.3})$$

$$\begin{aligned} J_{ijk} &= \int \frac{d^d \mathbf{q}}{(2\pi)^d} \frac{q_i q_j q_k}{(\mathbf{q}^2)^\alpha [(\mathbf{q} - \mathbf{k})^2]^\beta} \\ &= \frac{(\mathbf{k}^2)^{d/2-\alpha-\beta}}{(4\pi)^{d/2}} \frac{\Gamma(\alpha + \beta - d/2 - 1)}{\Gamma(\alpha)\Gamma(\beta)} \frac{\Gamma(d/2 - \alpha + 2)\Gamma(d/2 - \beta)}{\Gamma(d - \alpha - \beta + 3)} \\ &\quad \times \left[(d/2 - \alpha + 2)(\alpha + \beta - d/2 - 1)k_i k_j k_k + (d/2 - \beta) \frac{\mathbf{k}^2}{2} (\delta_{ij} k_k + \delta_{jk} k_i + \delta_{ik} k_j) \right] \end{aligned} \quad (\text{A.4})$$

$$\begin{aligned} J_{ijkl} &= \int \frac{d^d \mathbf{q}}{(2\pi)^d} \frac{q_i q_j q_k q_l}{(\mathbf{q}^2)^\alpha [(\mathbf{q} - \mathbf{k})^2]^\beta} = \frac{(\mathbf{k}^2)^{d/2-\alpha-\beta}}{(4\pi)^{d/2}} \frac{\Gamma(d/2 - \alpha + 2)\Gamma(d/2 - \beta)}{\Gamma(d - \alpha - \beta + 4)} \\ &\quad \times \frac{\Gamma(\alpha + \beta - d/2 - 2)}{\Gamma(\alpha)\Gamma(\beta)} \left[(d/2 - \beta)(d/2 - \beta + 1)(\delta_{ij} \delta_{kl} + \delta_{ik} \delta_{jl} + \delta_{il} \delta_{jk}) \frac{(\mathbf{k}^2)^2}{4} \right. \\ &\quad \left. + (\delta_{ij} k_k k_l + \delta_{ik} k_j k_l + \delta_{il} k_j k_k + \delta_{jk} k_i k_l + \delta_{jl} k_i k_k + \delta_{kl} k_i k_j) \frac{\mathbf{k}^2}{2} \right. \\ &\quad \left. \times (\alpha + \beta - d/2 - 2)(d/2 - \alpha + 2)(d/2 - \beta) \right. \\ &\quad \left. + k_i k_j k_k k_l (\alpha + \beta - d/2 - 2)(\alpha + \beta - d/2 - 1)(d/2 - \alpha + 2)(d/2 - \alpha + 3) \right] \end{aligned} \quad (\text{A.5})$$

As noticed in [8] the above integrals (A.2)-(A.5) of vector nature can be reduced to a scalar integral (A.1) on the basis of their transformation properties under rotations. Yet such a reduction becomes involved when the rank of the tensor under consideration increases, and therefore we choose to list all those which were relevant to this work.

In order to evaluate the above integrals we proceed as follows. We first apply the generalized Feynman parametrization [37]

$$\prod_{i=1}^N \frac{1}{A_i^{m_i}} = \int_0^1 \prod_{i=1}^N dx_i \delta\left(\sum x_i - 1\right) \frac{\prod x_i^{m_i-1}}{[\sum x_i A_i]^{\sum m_i}} \frac{\Gamma(m_1 + m_2 + \dots + m_N)}{\Gamma(m_1) \dots \Gamma(m_N)} \quad (\text{A.6})$$

with $N = 2$ and $m_1 = \alpha$, $m_2 = \beta$. Next we integrate over one of the Feynman parameters, e.g. x_2 , and subsequently redefine the undetermined wave-number $\mathbf{q} \rightarrow \mathbf{q} + x_1 \mathbf{k}$.

Now, in order to integrate over \mathbf{q} , we build on the following formula

$$\int \frac{d^d \mathbf{q}}{(2\pi)^d} \frac{1}{(z \mathbf{q}^2 + \Delta)^n} = \frac{z^{-d/2}}{(4\pi)^{d/2}} \frac{\Gamma(n - d/2)}{\Gamma(n)} \Delta^{d/2-n}, \quad (\text{A.7})$$

computed by means of dimensional regularization. Thus, for instance, differentiating it with respect to z a definite number of times and setting $z = 1$, one obtains

$$\begin{aligned} \int \frac{d^d \mathbf{q}}{(2\pi)^d} \frac{\mathbf{q}^2}{(\mathbf{q}^2 + \Delta)^n} &= \frac{d/2}{(4\pi)^{d/2}} \frac{\Gamma(n - d/2 - 1)}{\Gamma(n)} \Delta^{d/2-n+1}, \\ \int \frac{d^d \mathbf{q}}{(2\pi)^d} \frac{(\mathbf{q}^2)^2}{(\mathbf{q}^2 + \Delta)^n} &= \frac{d(d+2)}{4(4\pi)^{d/2}} \frac{\Gamma(n - d/2 - 2)}{\Gamma(n)} \Delta^{d/2-n+2}. \end{aligned} \quad (\text{A.8})$$

As a final step we integrate over x_1 .

Another set of useful identities is related to the following d -dimensional Fourier transform

$$\int \frac{d^d \mathbf{k}}{(2\pi)^d} \frac{e^{i\mathbf{k}\mathbf{r}}}{(\mathbf{k}^2)^\alpha} = \frac{1}{(4\pi)^{d/2}} \frac{\Gamma(d/2 - \alpha)}{\Gamma(\alpha)} \left(\frac{\mathbf{r}^2}{4}\right)^{\alpha-d/2}. \quad (\text{A.9})$$

Differentiating it with respect to \mathbf{r} yields

$$\begin{aligned} \int \frac{d^d \mathbf{k}}{(2\pi)^d} \frac{\mathbf{k}_i}{(\mathbf{k}^2)^\alpha} e^{i\mathbf{k}\mathbf{r}} &= i x_i \frac{\Gamma(d/2 - \alpha + 1)}{2(4\pi)^{d/2} \Gamma(\alpha)} \left(\frac{\mathbf{r}^2}{4}\right)^{\alpha-d/2-1}, \\ \int \frac{d^d \mathbf{k}}{(2\pi)^d} \frac{\mathbf{k}_i \mathbf{k}_j}{(\mathbf{k}^2)^\alpha} e^{i\mathbf{k}\mathbf{r}} &= \frac{\Gamma(d/2 - \alpha + 1)}{(4\pi)^{d/2} \Gamma(\alpha)} \left(\frac{\delta_{ij}}{2} + (\alpha - d/2 - 1) \frac{x_i x_j}{\mathbf{r}^2}\right) \left(\frac{\mathbf{r}^2}{4}\right)^{\alpha-d/2-1} \end{aligned} \quad (\text{A.10})$$

$$\begin{aligned} \int \frac{d^d \mathbf{k}}{(2\pi)^d} \frac{\mathbf{k}_i \mathbf{k}_j \mathbf{k}_l}{(\mathbf{k}^2)^\alpha} e^{i\mathbf{k}\mathbf{r}} &= \frac{i \Gamma(d/2 - \alpha + 2)}{16(4\pi)^{d/2} \Gamma(\alpha)} \left(\frac{\mathbf{r}^2}{4}\right)^{\alpha-d/2-3} \\ &\times [\mathbf{r}^2(\delta_{il} x_j + \delta_{jl} x_i + \delta_{ij} x_l) - (d - 2\alpha + 4) x_i x_j x_l], \end{aligned} \quad (\text{A.11})$$

$$\begin{aligned} \int \frac{d^d \mathbf{k}}{(2\pi)^d} \frac{\mathbf{k}_i \mathbf{k}_j \mathbf{k}_l \mathbf{k}_m}{(\mathbf{k}^2)^\alpha} e^{i\mathbf{k}\mathbf{r}} &= \frac{\Gamma(d/2 - \alpha + 3)}{32(4\pi)^{d/2} \Gamma(\alpha)} \left(\frac{\mathbf{r}^2}{4}\right)^{\alpha-d/2-4} [(d - 2\alpha + 6) x_i x_j x_l x_m \\ &- \mathbf{r}^2(\delta_{im} x_j x_l + \delta_{jm} x_i x_l + \delta_{lm} x_i x_j + \delta_{il} x_m x_j + \delta_{jl} x_i x_m + \delta_{ij} x_l x_m) \\ &+ \frac{(\mathbf{r}^2)^2}{(d - 2\alpha + 4)} (\delta_{il} \delta_{jm} + \delta_{jl} \delta_{im} + \delta_{ij} \delta_{lm})]. \end{aligned} \quad (\text{A.12})$$

References

- [1] S. Rowan and J. Hough, “Gravitational Wave Detection By Interferometry (Ground And Space),” *Living Rev. Rel.* **3**, 3 (2000). B. S. Sathyaprakash and B. F. Schutz, “Physics, Astrophysics and Cosmology with Gravitational Waves,” *Living Rev. Rel.* **12**, 2 (2009) [arXiv:0903.0338 [gr-qc]].

- [2] F. Pretorius, “Binary Black Hole Coalescence,” arXiv:0710.1338 [gr-qc].
- [3] L. Blanchet, “Gravitational radiation from post-Newtonian sources and inspiralling compact binaries,” *Living Rev. Rel.* **5**, 3 (2002), update: *Living Rev. Rel.* **9**, 4 (2006) [arXiv:gr-qc/0202016]. “Post-Newtonian theory and the two-body problem,” arXiv:0907.3596 [gr-qc].
- [4] G. Schafer, “Post-Newtonian methods: Analytic results on the binary problem,” arXiv:0910.2857 [gr-qc].
- [5] W. D. Goldberger and I. Z. Rothstein, “An effective field theory of gravity for extended objects,” *Phys. Rev. D* **73**, 104029 (2006) [arXiv:hep-th/0409156]. W. D. Goldberger, “Les Houches lectures on effective field theories and gravitational radiation,” arXiv:hep-ph/0701129.
- [6] B. Kol and M. Smolkin, “Classical Effective Field Theory and Caged Black Holes,” *Phys. Rev. D* **77**, 064033 (2008) [arXiv:0712.2822 [hep-th]].
- [7] B. Kol and M. Smolkin, “Non-Relativistic Gravitation: From Newton to Einstein and Back,” *Class. Quant. Grav.* **25**, 145011 (2008) [arXiv:0712.4116 [hep-th]].
- [8] J. B. Gilmore and A. Ross, “Effective field theory calculation of second post-Newtonian binary dynamics,” *Phys. Rev. D* **78**, 124021 (2008) [arXiv:0810.1328 [gr-qc]].
- [9] W. D. Goldberger and I. Z. Rothstein, “Dissipative effects in the world-line approach to black hole dynamics,” *Phys. Rev. D* **73**, 104030 (2006) [arXiv:hep-th/0511133].
- [10] B. Kol, “The Delocalized Effective Degrees of Freedom of a Black Hole at Low Frequencies,” *Gen. Rel. Grav.* **40**, 2061 (2008) [*Int. J. Mod. Phys. D* **17**, 2617 (2009)] [arXiv:0804.0187 [hep-th]].
- [11] T. Harmark, “Small black holes on cylinders,” *Phys. Rev. D* **69**, 104015 (2004) [arXiv:hep-th/0310259].
- [12] D. Gorbounov and B. Kol, “A dialogue of multipoles: Matched asymptotic expansion for caged black holes,” *JHEP* **0406**, 053 (2004) [arXiv:hep-th/0406002].
- [13] Y. Z. Chu, W. D. Goldberger and I. Z. Rothstein, “Asymptotics of d-dimensional Kaluza-Klein black holes: Beyond the newtonian approximation,” *JHEP* **0603**, 013 (2006) [arXiv:hep-th/0602016].
- [14] J. B. Gilmore, A. Ross and M. Smolkin, “Caged black hole thermodynamics: Charge, the extremal limit, and finite size effects,” *JHEP* **0909**, 104 (2009) [arXiv:0908.3490 [hep-th]].
- [15] R. A. Porto and I. Z. Rothstein, “The hyperfine Einstein-Infeld-Hoffmann potential,” *Phys. Rev. Lett.* **97**, 021101 (2006) [arXiv:gr-qc/0604099].
- [16] J. Steinhoff and G. Schafer, “Canonical formulation of self-gravitating spinning-object systems,” *Europhys. Lett.* **87**, 50004 (2009) [arXiv:0907.1967 [gr-qc]].
- [17] E. Barausse, E. Racine and A. Buonanno, “Hamiltonian of a spinning test-particle in curved spacetime,” arXiv:0907.4745 [gr-qc].
- [18] T. Damour and A. Nagar, “Relativistic tidal properties of neutron stars,” arXiv:0906.0096 [gr-qc]. T. Damour and O. M. Lecian, “On the gravitational polarizability of black holes,” *Phys. Rev. D* **80**, 044017 (2009) [arXiv:0906.3003 [gr-qc]].

- [19] T. Binnington and E. Poisson, “Relativistic theory of tidal Love numbers,” arXiv:0906.1366 [gr-qc].
- [20] R. Emparan, T. Harmark, V. Niarchos, N. A. Obers and M. J. Rodriguez, “The Phase Structure of Higher-Dimensional Black Rings and Black Holes,” JHEP **0710**, 110 (2007) [arXiv:0708.2181 [hep-th]].
- [21] R. Emparan, T. Harmark, V. Niarchos and N. A. Obers, “Essentials of Blackfold Dynamics,” arXiv:0910.1601 [hep-th].
- [22] Y. Z. Chu, “The n-body problem in General Relativity up to the second post-Newtonian order from perturbative field theory,” Phys. Rev. D **79**, 044031 (2009) [arXiv:0812.0012 [gr-qc]].
- [23] M. Headrick, S. Kitchen and T. Wiseman, “A new approach to static numerical relativity, and its application to Kaluza-Klein black holes,” arXiv:0905.1822 [gr-qc].
- [24] V. Cardoso, O. J. C. Dias and P. Figueras, “Gravitational radiation in $d > 4$ from effective field theory,” Phys. Rev. D **78**, 105010 (2008) [arXiv:0807.2261 [hep-th]].
- [25] C. R. Galley and M. Tiglio, “Radiation reaction and gravitational waves in the effective field theory approach,” Phys. Rev. D **79**, 124027 (2009) [arXiv:0903.1122 [gr-qc]].
- [26] J. S. Schwinger, “On the Green’s functions of quantized fields. I, II” Proc. Natl. Acad. Sci. **37**, 452 (1951); *ibid.* 455. F. J. Dyson, “The S-matrix in quantum electrodynamics,” Phys. Rev. D, **75** 1736 (1949).
- [27] K. Blagoev, F. Cooper, J. Dawson and B. Mihaila, “Schwinger-Dyson approach to non-equilibrium classical field theory,” Phys. Rev. D **64**, 125003 (2001) [arXiv:hep-ph/0106195].
- [28] M. Duetsch and K. Fredenhagen, “The master Ward identity and generalized Schwinger-Dyson equation in classical field theory,” Commun. Math. Phys. **243**, 275 (2003) [arXiv:hep-th/0211242].
- [29] T. Ledvinka, G. Schaefer and J. Bicak, “Relativistic Closed-Form Hamiltonian for Many-Body Gravitating Systems in the Post-Minkowskian Approximation,” Phys. Rev. Lett. **100**, 251101 (2008) [arXiv:0807.0214 [gr-qc]].
- [30] R. Alkofer and L. von Smekal, “The infrared behavior of QCD Green’s functions: Confinement, dynamical symmetry breaking, and hadrons as relativistic bound states,” Phys. Rept. **353**, 281 (2001) [arXiv:hep-ph/0007355].
- [31] T. Damour, P. Jaranowski and G. Schaefer, “Dimensional regularization of the gravitational interaction of point masses,” Phys. Lett. B **513**, 147 (2001) [arXiv:gr-qc/0105038].
L. Blanchet, T. Damour and G. Esposito-Farese, “Dimensional regularization of the third post-Newtonian dynamics of point particles in harmonic coordinates,” Phys. Rev. D **69**, 124007 (2004) [arXiv:gr-qc/0311052].
L. Blanchet, T. Damour, G. Esposito-Farese and B. R. Iyer, “Dimensional regularization of the third post-Newtonian gravitational wave generation from two point masses,” Phys. Rev. D **71**, 124004 (2005) [arXiv:gr-qc/0503044].
- [32] U. Cannella and R. Sturani, “Classical energy momentum tensor renormalisation via effective field theory methods,” arXiv:0808.4034 [gr-qc].
- [33] J. D. Bjorken and S. S. Drell, *Relativistic quantum fields*, ch.19 p.293, (McGraw-Hill, 1965).
- [34] C. Itzykson and J.-B. Zuber, *Quantum Field Theory*, ch. 10 p. 475, (McGraw-Hill, 1980).

- [35] D. Amati, M. Ciafaloni and G. Veneziano, “Effective action and all order gravitational eikonal at Planckian energies,” Nucl. Phys. B **403**, 707 (1993).
- [36] D. Amati, M. Ciafaloni and G. Veneziano, “Towards an S-matrix Description of Gravitational Collapse,” JHEP **0802**, 049 (2008) [arXiv:0712.1209 [hep-th]].
- [37] M. E. Peskin and D. V. Schroeder, “An Introduction To Quantum Field Theory,” Reading, USA: Addison-Wesley (1995) 842 p.